ASTRONOMY & ASTROPHYSICS
SUPPLEMENT SERIES

Astron. Astrophys. Suppl. Ser. **73,** 515-547 (1988)

Observations of the large scale radio structure in high redshift quasars

P. D. Barthel ([1,*]), G. K. Miley ([1,2,3]), R. T. Schilizzi ([4]) and C. J. Lonsdale ([5])

([1]) Leiden Observatory, P.O. Box 9513, NL-2300 RA Leiden, The Netherlands
([2]) Space Telescope Science Institute, Homewood Campus, Baltimore, MD 21218, U.S.A.
([3]) affiliated to the Astrophysics Division, Space Science Dept. of the European Space Agency, Noordwijk, The Netherlands
([4]) Netherlands Foundation for Radio Astronomy, P.O. Box 2, NL-7990 AA Dwingeloo, The Netherlands
([5]) MIT/NEROC Haystack Observatory, Westford, MA 01886, U.S.A.

Received October 21, accepted December 11, 1987

Summary. — Very Large Array (VLA) observations are presented of 105 high luminosity quasi-stellar radio sources with previously unknown radio structure, steep or unknown radio spectrum, and redshifts exceeding 1.5. The observations were made at 6 cm wavelength, and yielded radio maps at about 0.5 arcsec resolution. The maps indicate that many of these luminous high redshift quasars have distorted morphologies.

Key words : cosmology — quasars : general — radio continuum.

1. Introduction.

Quasars provide a unique set of beacons for tracing the evolution in the universe, since we can observe these objects out to distances of many billion light years. The small fraction of quasi-stellar objects which have detectable radio emission are particularly important in this respect, since measurements of their structures as a function of redshift provide *morphological* information about the cosmic evolution of extragalactic radio sources. Since aperture synthesis instruments became available in the sixties, many studies have been devoted to the morphology of extended extragalactic radio sources, associated with quasars (e.g., Macdonald and Miley, 1971 ; Miley, 1971 ; Wardle and Miley, 1974 ; Miley and Hartsuijker, 1978). Apart from the generally higher core flux density fraction, no important differences with powerful nearby radio galaxies have been found. See e.g., the reviews of Miley (1980) and Owen (1986).

When this project began in 1981, the radio morphologies of only about ten quasars with $z > 1.5$ were known. Their angular sizes appeared to be less than or of the order of 10 arseconds. Since these were mainly 3C sources, they were typically much more luminous than lower redshift sources, making it impossible to distinguish morphological properties which depend on redshift from those which depend on luminosity. Also, in order to make a useful comparison with low redshift quasars, angular resolution better than one arcsecond is required. When the VLA with its high sensitivity and subarcsecond resolution became available, we therefore started a new and extensive program to study the radio properties of quasars at high redshift. This paper describes our selection criteria, discusses the observations and data reduction procedures, and presents the results of this program in the form of radio maps for seventy-three sources with extended morphologies.

2. Sample selection and observations.

The high redshift quasars in our program were extracted from the compilation of Hewitt and Burbidge (1980), using the following selection criteria :

(1) redshift > 1.5 ;
(2) accessible to the VLA, $\delta_{1950} > -30°$;
(3) known to be a radio source ;
(4) since extended radio emission has a steep spectrum : steep radio spectrum : $\alpha^5_{1.4}$ or $\alpha^5_{0.408} \geq 0.6$ (where $S_\nu \propto \nu^{-\alpha}$), or unknown radio spectrum. Amongst the latter were many Molonglo (MC), Bologna (B), and Westerbork (W) quasars with only one measured spectral point ;
(5) unknown or poorly known radio structure.

The resulting sample consisted of 105 quasars with redshifts between 1.502 and 3.190. We observed this sample with the NRAO Very Large Array (Thompson

(*) now at Owens Valley Radio Observatory, Caltech 105-24, Pasadena, CA 91125, U.S.A.

Send offprint requests to : Dr. P. D. Barthel, Caltech 105-24, Pasadena, CA 91125, U.S.A.

et al., 1980) in its A-configuration at 4885 MHz frequency and 50 or 100 MHz bandwidth. The observations were made in snapshot mode during several observing sessions : February 27-28, 1982, August 21-22, 1983, February 26 and March 10, 1985, and April 27-29, 1986. Generally, the fields were observed for 5-8 min, but in several cases for 15-20 min. A few sources were observed during more than one session, in order to check the reliability of structure marginally detected in the first session. After standard calibration with external calibrators (3C 286 being the prime flux density calibrator), each field was mapped, cleaned, and self-calibrated, using standard algorithms. Generally two passes through the self-calibration step were made. This procedure yielded radio maps with dynamic range of typically 200 : 1, except for the weak sources for which the maps are thermal noise limited. The 3 σ noise level depends on the integration time and the dynamic range, and in general lies between 0.1 and 1 mJy per beam area, the latter being typically 0.5 arcsecond in diameter. Using the 5 GHz total flux densities obtained, the spectral indices $\alpha^5_{0.408}$ or $\alpha^5_{1.4}$ were derived for the sources with previously unknown radio spectrum. Since the observations were carried out in the high resolution (A-array) mode, the instrument is not sensitive to extended emission exceeding ~ 10 arcsec in angular size. Since furthermore extended emission usually has a steep radio spectrum, our observations of these high redshift radio sources may have missed extended low brightness emission in some cases. From comparison with existing and newly obtained data, we estimate this effect to be minor in extent, and refer to the comments on individual sources below. For many of the quasars the position of the associated optical QSO was not known with sufficient accuracy for useful comparison with our radio data. Using Palomar Observatory Sky Survey blue plates we measured the positions of these objects with the plate measuring machine at Leiden Observatory. Using the internal consistency of redundant reference stars, the accuracy of these measurements is estimated to be 0.3-0.6 arcsecond (standard error).

3. Results.

3.1 CONTOUR MAPS. — We present the results of this study in the form of radio contour maps, preceded by a table. This table I lists the quasars observed, with the quasar name according to the IAU convention in column 1, the radio source name or catalogue (column 2), the emission line redshift (column 3), the measured total 5 GHz flux density in mJy (column 4), the derived spectral index from 1.4 or 0.408 GHz to 5 GHz (column 5), a morphological classification (column 6) where an asterisk refers to the comments on individual sources below, and accurate positions for the associated optical QSO (columns 7 and 8). A number in column 9 indicates the reference to an optical position in the literature which appeared to have sufficient accuracy, and hence was not measured by us. The morphological classification in column 6 is such that MAP refers to the contour maps, U indicates an unresolved source, and SR indicates a slightly resolved radio source. In figures 1 to 73 we present contour maps of the total intensity in seventy-three quasars having radio morphologies exceeding one arcsecond in overall angular extent. Contour levels, peak brightness values, and restoring clean beam diameters for all the maps are given in the accompanying table II. Generally the restoring beam is 0.4-0.5 arcsec, but in several cases we show convolved maps (0.7-1.5 arcsec beam). The positions of the optical QSOs are marked with a + sign. For completeness, we list in table III the references to previously published maps of steep spectrum quasars at $z > 1.5$ which do not appear in table I.

3.2 COMMENTS ON INDIVIDUAL SOURCES. — 0032+423 : we identify a weak unresolved component with the core of this source ; a hotspot is responsible for the dominant emission.

0046−067 : The core radio emission in this source is most likely below our detection limit.

0109+176 : A lower resolution map of this source has been published by Feigelson *et al.* (1984).

0225−014 : A lower resolution map has been published by Downes *et al.* (1986) ; this map shows additional low brightness emission near the western lobe.

0404+177 : Our map solves the positional disagreement reported by Wills (1979) ; the feature at $04^h04^m36^s.55$ is the lobe of a D2 quasar, having a weak radio core at the position of the optical QSO.

0445+097 : The QSO is most likely identified with the bright eastern component.

0805+046 : MERLIN data at 18 cm, obtained by the authors, have shown that the weak feature NW of the quasar core is real : 0805+046 has an overall angular extent of 7 arcsec.

0808+289 : A low resolution map (Rogora *et al.*, 1986) confirms the earlier report (Fanti *et al.*, 1977), that the source is a triple with overall extent 34 arcsec.

0835+580 : Lonsdale and Barthel (1986a) recently provided extensive, multifrequency information on this source (3C 205), with special attention to the double hotspot in the southern lobe.

0836+195 : Saikia *et al.* (1984) detected a southern lobe in this source : 0836+195 is a triple source of 33 arcsec overall angular dimension.

0843+136 : We identify the eastern, unresolved component with the QSO ; the western component contains a very compact hotspot (Barthel, 1983).

0848+155 : From higher resolution observations we identify the western component with the QSO.

0856+124 : It is not clear which component is the core.

0941+261 : We identify the brightest (steep spectrum) component in this source with the QSO. A MERLIN map, obtained by the authors, shows that the curved jet continues for another two seconds of arc.

1153+317 : Additional high resolution maps can be found in Van Breugel *et al.* (1984).

1318+113 : Our VLA observations at 15 GHz have revealed a very weak core at the north-ernmost tip of the jet, near the position of the optical QSO.

1334+119 : The location of the core is not clear.

1354+258 : We have unambiguously identified the easternmost component of the jet with the QSO.

1356−201 : We find no radio emission at or around the position of the optical QSO (White *et al.*, 1979).

1629+120 : We have unambiguously identified the westermost component with the QSO.

1658+575 : Comparison of our map with an 1667 MHz MERLIN map (Shone, 1985) shows that the unresolved component at δ_{1950} 57°35′53.″9 should be identified with the QSO : 1658+575 is an asymmetric triple source.

1702+298 : This very distorted source has been subject of extensive investigations (Lonsdale and Barthel, 1986b).

2025+117 : The map of this very large (55 arcsec) quasar is shown, but it is not clear if the identification is correct ; Mitton *et al.* (1977) give RA_{1950} $20^h25^m55^s.36$, δ_{1950} + 11°45′27.″0, but we find no optical object at this position ; three optical objects in a crowded field are within seven arcseconds from the brightest radio component.

2222+051 : From our accurate position, and spectral information for the components (obtained with additional MERLIN and VLA maps) we identify the central component with the QSO.

2338+042 : We have identified the central component with the QSO (Barthel and Lonsdale, 1983).

4. Discussion.

Inspection of table I shows that the sources having a flat spectrum ($0 < \alpha < 0.5$) or an inverted spectrum ($\alpha < 0$) are found to be unresolved, as expected (see e.g., Kellermann and Pauliny-Toth, 1981). The converse is certainly not true : several unresolved steep spectrum cores (SSCs, e.g., Van Breugel *et al.*, 1984) were detected. The maps contain a wealth of information, which will be analysed in forthcoming papers. Due to the selection criteria, all the quasars observed have high intrinsic luminosities, which for nearby radio galaxies and quasars would indicate membership of the Fanaroff and Riley class II of edge-brightened triple sources. However, inspection of the maps indicates a deficit of such morphologies. Indeed, many of the quasars have very peculiar morphologies : in particular, bending with respect to the radio core is frequently present. By comparing the high redshift morphological data obtained in the present study with morphological data for lower redshift steep spectrum quasars, Barthel and Miley (1987) find luminosity-independent linear size evolution $\propto (1+z)^{-k}$, with $k = 1.5 - 2$ (for $q_0 = 0.5$). They also show that the observed high redshift bending is an epoch-dependent source property, and propose a link with the epoch of galaxy formation to explain the observed high redshift morphologies. It is of interest to note that the two quasars at $z > 3$ (0731+653 and 0938+119) display unresolved morphologies and flat radio spectra, in agreement with the general trend for quasars at such very high redshift (Barthel, 1986). The highest redshift quasar showing morphology on the arcsec scale appears to be 0941+261 (OK 270) at $z = 2.910$. Its very distorted jet takes over from 2338+042 (4C 04.81, Barthel and Lonsdale, 1983) as being the highest redshift jet.

A number of papers on individual members or subgroups of the sample have been published or are in preparation. Lonsdale and Barthel (1986b) presented higher resolution VLA, MERLIN, and *VLBI* maps of the very distorted quasar 1702+298 (4C 29.50), and proposed that a strong interaction between the radio jet and the inner galactic environment is responsible for the observed distorted morphology. Lonsdale and Barthel (1987) discuss some quasars from the present sample which display weak cores and strong jets, and argue that the observed spread in core/jet flux ratios in general does not constrain the flow velocities in core and jet, contrary to earlier claims. Barthel *et al.* (1988) discuss the presence and interrelation of both radio jet distortion and strong associated absorption lines in 2338+042 (4C 04.81), and present arguments for a common origin.

Most of these intriguing, distant quasars require more detailed radio and optical studies. Extensive projects of high dynamic range mapping at 20 and 6 cm, and higher resolution mapping at 2 cm wavelength (both including polarization), as well as optical spectroscopy and imaging are in progress. Forthcoming papers on the radio mapping programs will contain extensive data on source component parameters, and subsequent analysis.

Acknowledgements.

We thank the VLA staff for help with the observations, K. W. C. Lugtenborg for his assistance with the Leiden VLA reduction package, and F. van Roermund and A. Grensemann for help with the data reduction and the optical identifications. The NRAO VLA is operated by Associated Universities, Inc., under contract with the National Science foundation. PDB acknowledges support by the Netherlands Organization for the Advancement of Pure Research (ZWO), through ASTRON grant 19-23-13, and also acknowledges travel support from the Leids Kerkhoven-Bosscha Fonds. OVRO is financially supported by the NSF, under grant 85-09822.

References

ARGUE, A. N., KENWORTHY, C. M. : 1972, *Mon. Not. R. Astron. Soc.* **160,** 197.

BALDWIN, J. A., SMITH, H. E., BURBIDGE, E. M., HAZARD, C., MURDOCH, H. S., JAUNCEY, D. L. : 1976, *Astrophys. J. Lett.* **206,** 283.

BARTHEL, P. D. : 1983, *Astron. Astrophys.* **126,** 16.
BARTHEL, P. D. : 1986, in *IAU Symp.* No. **119,** Quasars, Eds Swarup and Kapahi (Dordrecht, Reidel) p. 181.
BARTHEL, P. D., LONSDALE, C. J. : 1983, *Mon. Not. R. Astron. Soc.* **205,** 395.
BARTHEL, P. D., MILEY, G. K. : 1987, submitted to *Nature*.
BARTHEL, P. D., TYTLER, D. R., LONSDALE, C. J., MILEY, G. K. : 1988, in preparation.
COHEN, A. M., PORCAS, R. W., BROWNE, I. W. A., DAINTREE, E. J., WALSH, D. : 1977, *Mem. R. Astron. Soc.* **81,** 1.
DE RUITER, H. R., WILLIS, A. G., ARP, H. C. : 1977, *Astron. Astrophys. Suppl. Ser.* **28,** 11.
DOWNES, A. J. B., PEACOCK, J. A., SAVAGE, A., CARRIE, D. R. : 1986, *Mon. Not. R. Astron. Soc.* **218,** 31.
FANTI, C., FANTI, R., FICARRA, A., FORMIGGINI, L., GIOVANNINI, G., LARI, C., PADRIELLI, L. : 1975, *Astron. Astrophys. Suppl. Ser.* **19,** 143.
FANTI, C., FANTI, R., FORMIGGINI, L., LARI, C., PADRIELLI, L. : 1977, *Astron. Astrophys. Suppl. Ser.* **28,** 351.
FEIGELSON, E. D., ISOBE, I., KEMBHAVI, A. : 1984, *Astron. J.* **89,** 1464.
HAZARD, C. : 1983, private communication.
HAZARD, C., MURDOCH, H. S. : 1977, *Aust. J. Phys. Astrophys. Suppl. Ser.* **42.**
HEWITT, A., BURBIDGE, G. : 1980, *Astrophys. J. Suppl. Ser.* **43,** 57.
HOSKINS, D. G., MURDOCH, H. S., HAZARD, C., JAUNCEY, D. L. : 1972, *Aust. J. Phys.* **25,** 559.
HOSKINS, D. G., MURDOCH, H. S., ADGIE, R. L., CROWTHER, J. H., GENT, H. : 1974, *Mon. Not. R. Astron. Soc.* **166,** 235.
HUNSTEAD, R. W., MURDOCH, H. S., SHOBBROOK, R. R. : 1978, *Mon. Not. R. Astron. Soc.* **185,** 149.
JENKINS, C. J., POOLEY, G. G., RILEY, J. M. : 1977, *Mem. R. Astron. Soc.* **84,** 61.
KELLERMANN, K. I., PAULINY-TOTH, I. I. K. : 1981, *Ann. Rev. Astron. Astrophys.* **19,** 373.
KRISTIAN, J., SANDAGE, A. : 1970, *Astrophys. J.* **162,** 391.
LONSDALE, C. J., BARTHEL, P. D. : 1986a, *Astron. J.* **92,** 12.
LONSDALE, C. J., BARTHEL, P. D. : 1986b, *Astrophys. J.* **303,** 617.
LONSDALE, C. J., BARTHEL, P. D. : 1987, *Astron. J.* **94,** 1487.
MACDONALD, G. H., MILEY, G. K. : 1971, *Astrophys. J.* **164,** 237.
MERKELIJN, J. K. : 1969, *Aust. J. Phys.* **22,** 237.
MILEY, G. K., HARTSUIJKER, A. P. : 1978, *Astron. Astrophys. Suppl. Ser.* **34,** 129.
MILEY, G. K. : 1971, *Mon. Not. R. Astron. Soc.* **152,** 477.
MILEY, G. : 1980, *Ann. Rev. Astron. Astrophys.* **18,** 165.
MITTON, S., HAZARD, C., WHELAN, J. A. J. : 1977, *Mon. Not. R. Astron. Soc.* **179,** 589.
MURDOCH, H. S., CRAWFORD, D. F. : 1977, *Mon. Not. R. Astron. Soc.* **180,** 41 P.
MURDOCH, H. S., SANITT, N. : 1979, *Aust. J. Phys.* **32,** 511.
OWEN, F. N. : 1986, in *IAU Symp.* No. **119,** Quasars, Eds Swarup and Kapahi (Dordrecht, Reidel) p. 173.
PORCAS, R. W., URRY, C. M., BROWNE, I. W. A., COHEN, A. M., DAINTREE, E. J., WALSH, D. : 1977, *Mon. Not. R. Astron. Soc.* **191,** 607.
RILEY, J. M., POOLEY, G. K. : 1975, *Mem. Roy. Astron. Soc.* **80,** 93.
ROGORA, A., PADRIELLI, L., DE RUITER, H. R. : 1986, *Astron. Astrophys. Suppl. Ser.* **64,** 557.
SAIKIA, D. J., SHASTRI, P., SINHA, R. P., KAPAHI, V. K., SWARUP, G. : 1984, *J. Astrophys. Astron.* **5,** 429.
SHIMMINS, A. J., BOLTON, J. G., WALL, J. V. : 1975, *Aust. J. Phys. Astrophys. Suppl. Ser.* **34,** 63.
SHONE, D. L. : 1985, Ph. D. thesis, Victoria University of Manchester.
STOCKE, J. T., BURNS, J. O., CHRISTIANSEN, W. A. : 1985, *Astrophys. J.* **299,** 799.
SWARUP, G., SINHA, R. P., SAIKIA, D. J. : 1982, *Mon. Not. R. Astron. Soc.* **201,** 393.
THOMPSON, A. R., CLARK, B. G., WADE, C. M., NAPIER, P. J. : 1980, *Astrophys. J. Suppl. Ser.* **44,** 151.
VAN BREUGEL, W., MILEY, G., HECKMAN, T. : 1984, *Astron. J.* **89,** 5.
WARDLE, J. F. C., MILEY, G. K. : 1974, *Astron. Astrophys.* **30,** 305.
WHITE, G. L., MURDOCH, H. S., HUNSTEAD, R. W. : 1979, *Mon. Not. R. Astron. Soc.* **192,** 545.
WILLIS, A. G., DE RUITER, H. R. : 1977, *Astron. Astrophys. Suppl. Ser.* **29,** 103.
WILLS, B. J. : 1976, *Astron. J.* **81,** 1031.
WILLS, D. : 1978, *Mon. Not. R. Astron. Soc.* **184,** 559.
WILLS, D. : 1979, *Astrophys. J. Suppl. Ser.* **39,** 291.
WILLS, D., WILLS, B. J. : 1974, *Astrophys. J.* **190,** 271.
WILLS, D., WILLS, B. J. : 1976, *Astrophys. J. Suppl. Ser.* **31,** 143.
WILLS, B. J., WILLS, D., DOUGLAS, J. N. : 1973, *Astron. J.* **78,** 521.

TABLE I. — *The high redshift quasar sample.*

QUASAR	RADIO SOURCE	z	S_{5GHz}	α	MORPH.	R.A.(1950)	DEC.(1950)	REFS.
0032+423	4C 42.01	1.588	120	1.0	MAP*	$00^h32^m23^s.33$	+42°21′49″.3	
0033+079	4C 08.04	1.578	130	1.2	MAP	00 33 40.96	+07 58 34.0	
0038−019	4C −02.04	1.690	280	1.1	MAP	00 38 52.62	−01 59 42.7	
0044−055	4C −05.03	1.869	140	0.8	MAP	00 44 12.01	−05 38 23.8	21
0045−000	PKS	1.536	100	0.1	U	00 45 45.38	−00 01 24.5	
0046−067	4C −06.04	2.063	140	0.8	MAP*	00 46 26.05	−06 44 49.9	
0051+291	4C 29.01	1.828	240	0.6	MAP	00 51 02.11	+29 08 51.2	
0054−006	PKS	2.795	240	−1.2	U	00 54 43.40	−00 40 43.0	
0109+176	4C 17.09	2.157	120	1.3	MAP*	01 09 09.62	+17 37 56.1	25
0119−046	4C −04.04	1.948	715	0.5	MAP	01 19 55.90	−04 37 07.5	
0206+293	B2	2.195	300	0.3	U	02 06 14.97	+29 18 34.7	21
0209−204	MC	1.823	105	0.4	U	02 09 42.60	−20 28 14.1	19
0225−014	4C −01.11	2.037	150	1.1	MAP*	02 25 35.04	−01 29 03.2	
0238+100	MC5	1.816	70	1.1	MAP	02 38 40.70	+10 05 59.5	
0316−203	MC	2.880	40	0.6	U	03 16 10.21	−20 23 12.0	19
0352+123	4C 12.17	1.616	230	1.0	MAP	03 52 59.25	+12 23 03.5	23
0404+177	4C 17.22	1.712	180	1.1	MAP*	04 04 36.15	+17 42 52.5	23
0407−199	MC	1.986	120	0.3	U	04 07 28.10	−19 55 49.9	19
0424−131	PKS	2.165	330	0.9	U	04 24 47.85	−13 09 33.4	
0445+097	4C 09.17	2.110	390	0.8	MAP*	04 45 37.12	+09 45 37.2	
0549−213	MC	2.245	190	0.8	MAP	05 49 50.56	−21 20 29.6	10
0553−205	MC	1.544	60	0.8	MAP	05 53 09.99	−20 30 19.7	
0730+257	4C 25.21	2.686	230	0.8	MAP	07 30 05.48	+25 42 54.8	22
0730+659	W1	1.937	30	0.8	MAP	07 30 17.96	+65 59 39.0	4
0731+653	W1	3.035	35	0.0	U	07 31 34.26	+65 19 49.8	
0747+613	OI 680	2.492	350	0.8	SR	07 47 50.17	+61 20 06.0	3
0751+298	4C 29.27	2.106	150	0.8	MAP	07 51 50.96	+29 49 50.7	25
0758+120	MC5	2.660	50	0.8	MAP	07 58 14.49	+12 01 43.3	2
0802+103	3C 191	1.956	490	1.1	MAP	08 02 03.80	+10 23 58.1	
0805+046	4C 05.34	2.877	340	0.4	MAP*	08 05 19.17	+04 41 20.0	11
0808+289	B2	1.910	50	0.5	U*	08 08 32.18	+28 54 02.5	5
0824+110	MC5	2.278	170	0.0	U	08 24 22.39	+11 02 19.4	2
0830+115	MC5	2.974	340	0.2	U	08 30 29.94	+11 33 52.9	2
0831+101	MC5	1.760	35	0.3	MAP	08 31 57.57	+10 08 16.5	
0835+580	3C 205	1.534	600	1.1	MAP*	08 35 10.02	+58 04 51.4	1
0836+195	4C 19.31	1.691	160	0.7	MAP*	08 36 15.00	+19 32 24.6	11
0843+136	4C 13.39	1.875	180	0.8	MAP*	08 43 01.35	+13 39 57.4	
0848+155	OJ 180	2.101	220	0.7	MAP*	08 48 04.36	+15 33 30.6	21
0856+124	MC5	1.760	45	0.8	MAP*	08 56 49.55	+12 28 17.1	
0926+117	4C 11.32	1.754	140	0.9	MAP	09 26 01.06	+11 47 32.4	11
0927+217	W2	1.830	35	0.1	U	09 27 53.07	+21 42 31.7	
0938+119	MC5	3.190	180	0.2	U	09 38 31.75	+11 59 12.6	2
0941+261	OK 270	2.910	350	0.8	MAP*	$09^h41^m50^s.22$	+26°08′32″.0	25
0945+114	MC5	1.760	220	0.0	U	09 45 04.76	+11 27 51.0	
0959+105	MC5	1.530	350	0.0	U	09 59 17.86	+10 30 19.0	
1023+067	3C 243	1.699	220	1.2	MAP	10 23 55.15	+06 42 50.7	11
1045+604	4C 60.15	1.722	400	0.5	U	10 45 23.10	+60 24 37.3	24
1055+499	5C 02.56	2.390	100	0.8	MAP	10 55 17.73	+49 55 39.7	
1104+728	W1	2.100	450	−0.2	U	11 04 18.10	+72 48 49.8	20
1126+101	PKS	1.515	375	0.5	MAP	11 26 38.7	+10 08 32	8
1148+568	W1	1.782	45	0.3	U	11 48 07.63	+56 49 36.9	
1153+317	4C 31.38	1.557	950	0.9	MAP*	11 53 44.08	+31 44 46.85	12
1153+534	W1	1.750	10	0.0	SR	11 53 42.84	+53 25 26.8	4
1157+532	W2	1.997	240	0.2	U	11 57 37.26	+53 17 28.4	4
1158+122	MC2	2.018	20	0.7	MAP	11 58 22.21	+12 14 00.4	
1207+398	W3	2.334	15	0.4	U	12 07 11.57	+39 53 23.0	
1214+106	MC2	1.884	40	1.0	MAP	12 14 28.42	+10 36 32.6	
1221+114	MC2	1.755	120	0.8	MAP	12 21 47.41	+11 23 59.6	
1225+317	B2	2.230	440	−0.2	U	12 25 55.94	+31 45 12.6	5
1226+105	MC2	2.296	190	1.0	MAP	12 26 04.61	+10 35 16.4	6
1308+182	4C 18.36	1.689	110	1.0	MAP	13 08 29.47	+18 15 33.8	26
1311−270	PKS	2.195	180	0.9	MAP	13 11 02.90	−27 00 55.9	
1318+113	4C 11.45	2.171	800	0.8	MAP*	13 18 49.68	+11 22 31.4	11
1323+655	4C 65.15	1.618	180	1.0	MAP	13 23 48.49	+65 30 46.6	3
1331+170	MC3	2.081	800	−0.1	U	13 31 10.1	+17 04 25	7
1334+119	MC2	1.760	120	0.8	MAP*	13 34 41.3	+11 55 29	7
1345+584	4C 58.27	2.039	200	0.8	MAP	13 45 55.97	+58 27 36.7	
1354+258	PKS	2.032	90	0.7	MAP*	13 54 48.40	+25 52 00.8	
1356−201	MC	1.970			*	13 56 54.95	−20 09 38.8	16
1448−232	PKS	2.221	370	0.5	U	14 48 09.2	−23 17 04	14
1456+092	MC	1.991	270	0.7	MAP	14 56 56.98	+09 16 01.8	25
1511+103	MC2	1.546	40	1.1	MAP	15 11 04.5	+10 22 15	7
1540+180	4C 18.43	1.662	250	0.6	MAP	15 40 03.62	+18 05 38.3	21
1554−203	MC	1.945	60	0.8	MAP	15 54 26.13	−20 20 34.8	19
1557−199	MC	1.590	20	0.8	MAP	15 57 16.13	−19 59 15.3	19
1559+173	4C 17.65	1.944	280	0.7	MAP	15 59 04.63	+17 22 36.5	25
1602−001	4C −00.63	1.625	380	0.8	MAP	16 02 22.0	−00 11 01	12
1602+576	4C 57.27	2.850	400	0.6	U	16 02 53.92	+57 39 01.9	16
1629+120	4C 12.59	1.782	740	0.7	MAP*	16 29 24.51	+12 02 24.4	
1629+680	4C 68.18	2.475	370	0.7	U	16 29 50.74	+68 03 39.1	3
1634+176	MC3	1.897	100	1.2	MAP	16 34 02.8	+17 41 10	7
1658+575	4C 57.29	2.173	110	1.5	MAP*	16 58 53.44	+57 35 52.4	3
1702+298	4C 29.50	1.927	570	0.8	MAP*	17 02 10.51	+29 51 04.8	
1732+160	4C 16.49	1.880	250	1.2	MAP	17 32 27.87	+16 02 27.3	25

Astronomy and Astrophysics n° 3-88 June. — 11

1988A&AS...73..515B

TABLE I *(continued)*.

QUASAR	RADIO SOURCE	z	S_{5GHz}	α	MORPH.	R.A.(1950)	DEC.(1950)	REFS.
1801+010	PKS	1.522	1150	0.1	U	$18^h01^m43^s.37$	$+01°01'19''.1$	9
1816+475	4C 47.48	2.225	150	1.1	MAP	18 16 58.70	+47 35 26.9	3
1857+566	4C 56.28	1.595	230	1.1	MAP	18 57 31.70	+56 41 45.8	3
2025+117	MC2	1.920	40	0.9	MAP*	20 25 54.30	+11 45 30.3	
2146−133	PKS	1.800	490	0.9	MAP	21 46 46.35	−13 18 26.4	
2149+212	4C 21.59	1.534	370	0.6	MAP	21 49 26.11	+21 16 06.9	17
2150+053	4C 05.81	1.979	310	1.1	MAP	21 50 54.12	+05 22 08.5	
2156+297	4C 29.64	1.753	450	0.8	MAP	21 56 27.72	+29 44 46.1	17
2158+101	4C 10.67	1.730	200	0.8	MAP	21 58 48.97	+10 09 19.3	
2209+152	MC3	1.502	70	0.8	MAP	22 09 07.85	+15 15 38.2	
2222+051	4C 05.84	2.323	240	0.9	MAP*	22 22 43.50	+05 11 53.4	
2223+210	PKS	1.960	1050	0.7	MAP	22 23 14.75	+21 02 50.0	
2248+192	4C 19.74	1.806	250	1.1	MAP	22 48 06.19	+19 15 25.1	
2249+185	3C 454.0	1.757	800	0.8	MAP	22 49 07.74	+18 32 43.9	11
2251+244	4C 24.61	2.328	870	0.6	SR	22 51 44.32	+24 29 24.7	17
2322+110	MC2	1.965	120	0.5	U	23 22 47.09	+11 02 09.0	
2332+489	OZ 453.7	1.534	130	1.3	MAP	23 32 17.90	+48 58 44.0	
2338+042	4C 04.81	2.594	450	1.0	MAP*	23 38 24.66	+04 14 37.2	
2345+061	4C 06.76	1.546	330	0.7	MAP	23 45 58.40	+06 08 18.7	
2353+154	MC3	1.801	500	0.6	U	23 53 20.1	+15 24 45	18
2354+144	4C 14.85	1.810	390	1.0	MAP	23 54 44.85	+14 29 27.2	

References

1. Argue & Kenworthy (1972)
2. Baldwin *et al.* (1976)
3. Cohen *et al.* (1977)
4. De Ruiter *et al.* (1977)
5. Fanti *et al.* (1975)
6. Hazard (1983)
7. Hazard & Murdoch (1977)
8. Hoskins *et al.* (1972)
9. Hoskins *et al.* (1974)
10. Hunstead *et al.* (1978)
11. Jenkins *et al.* (1977)
12. Kristian & Sandage (1970)
13. Merkelijn (1969)
14. Murdoch & Crawford (1977)
15. Murdoch & Sanitt (1979)
16. Porcas *et al.* (1980)
17. Riley & Pooley (1975)
18. Shimmins *et al.* (1975)
19. White *et al.* (1979)
20. Willis & De Ruiter (1977)
21. Wills (1976)
22. Wills (1978)
23. Wills (1979)
24. Wills & Wills (1974)
25. Wills & Wills (1976)
26. Wills *et al.* (1973)

TABLE II. — *Map parameters.*

QUASAR	CONTOUR VALUES (percentage of peak brightness)	PEAK (mJy/beam)	BEAM (arcsec)
0032+423	0.25, 0.50, 1.0, 1.5, 2.0, 2.5, 5, 10, 15, 20, 30, 50, 70, 90	78	0.70
0033+079	1.0, 1.5, 2.0, 2.5, 5, 10, 15, 20, 30, 50, 70, 90	40	0.60
0038−019	0.5, 1, 2, 4, 8, 15, 30, 50, 70, 90	54	0.40
0044−055	0.9, 1.4, 1.9, 2.4, 5, 10, 15, 20, 35, 50, 65, 80, 95	91	0.50
0046−067	1.0, 1.5, 2.0, 2.5, 5, 10, 15, 20, 30, 45, 60, 75, 90	66	0.40
0051+291	1, 2, 3, 5, 10, 15, 20, 35, 50, 65, 80, 95	135	0.40
0109+176	2.0, 2.5, 3.0, 3.5, 5, 10, 15, 20, 35, 50, 65, 80, 95	31	0.40
0119−046	0.5, 2.0, 3.5, 5, 10, 15, 20, 35, 50, 65, 80, 95	585	0.50
0225−014	1.0, 1.5, 2.0, 2.5, 5, 10, 15, 20, 35, 50, 65, 80, 95	85	1.00
0238+100	5.0, 7.5, 10.0, 12.5, 15, 20, 25, 30, 40, 50, 60, 70, 80, 90	21	1.20
0352+123	0.7, 1.5, 3, 6, 12, 20, 30, 50, 70, 90	111	0.40
0404+177	2, 2.5, 3, 5, 10, 20, 30, 50, 70, 90	67	0.40
0445+097	1.0, 1.5, 2.0, 2.5, 5, 10, 20, 35, 50, 65, 80, 95	159	0.40
0549−213	1.0, 1.5, 2.0, 2.5, 5, 10, 15, 20, 35, 50, 65, 80, 95	143	0.60
0553−205	0.5, 1.0, 1.5, 2.0, 2.5, 5, 10, 15, 20, 30, 50, 70, 90	45	0.70
0730+257	1.5, 2.0, 2.5, 5, 10, 15, 20, 30, 50, 70, 90	25	0.38
0730+659	2.5, 5.0, 7.5, 10.0, 12.5, 15, 20, 25, 30, 40, 50, 60, 70, 80, 90	14	1.10
0751+298	1.0, 1.5, 2.0, 2.5, 5, 10, 15, 20, 30, 45, 60, 75, 90	72	0.40
0758+120	2.0, 2.5, 3.0, 3.5, 5, 10, 15, 20, 35, 50, 65, 80, 95	33	0.50
0802+103	1.0, 1.5, 2.0, 2.5, 5, 10, 15, 20, 35, 50, 65, 80, 95	90	0.40
0805+046	0.8, 1.3, 1.8, 2.3, 5, 10, 15, 20, 35, 50, 65, 80, 95	250	0.50
0831+101	5, 10, 15, 20, 25, 35, 50, 65, 80, 95	10	1.00
0835+580	0.8, 1.4, 2.0, 2.6, 3.2, 3.8, 4.4, 5, 10, 15, 20, 35, 50, 65, 80, 95	166	0.50
0836+195	1.0, 1.5, 2.0, 2.5, 5, 10, 20, 35, 50, 65, 80, 95	75	0.40
0843+136	0.7, 1.2, 1.7, 2.2, 2.7, 5, 10, 15, 20, 35, 50, 65, 80, 95	97	0.40
0848+155	0.5, 1.0, 1.5, 2.0, 2.5, 5, 10, 15, 20, 30, 45, 60, 75, 90	112	0.40
0856+124	2, 4, 6, 8, 10, 15, 20, 25, 30, 40, 55, 70, 85, 90	19	0.50
0926+117	1.0, 1.5, 2.0, 2.5, 5, 10, 15, 20, 35, 50, 65, 80, 95	85	0.50
0941+261	0.5, 1.0, 1.5, 2.0, 2.5, 5, 10, 15, 20, 30, 45, 60, 75, 90	244	0.40
1023+067	1, 2, 3, 4, 5, 10, 15, 20, 25, 30, 45, 60, 75, 90	50	0.40
1055+499	1.0, 1.5, 2.0, 2.5, 5, 10, 15, 20, 35, 50, 65, 80, 95	62	0.40
1126+101	0.75, 1.25, 1.75, 2.25, 5, 10, 15, 20, 35, 50, 65, 80, 95	203	0.50
1153+317	0.25, 0.50, 1.0, 1.5, 2, 5, 10, 15, 20, 30, 50, 70, 90	592	0.41
1158+122	3.0, 3.5, 4, 5, 6, 7, 10, 15, 20, 35, 50, 65, 80, 95	15	0.50
1214+106	7.5, 12.5, 17.5, 22.5, 30, 40, 50, 60, 70, 80, 90	11	1.00
1221+114	0.6, 1.1, 1.6, 2.1, 2.6, 5, 10, 15, 20, 35, 50, 65, 80, 95	75	0.40
1226+105	1.1, 1.6, 2.1, 2.6, 5, 10, 15, 20, 35, 50, 65, 80, 95	53	0.40
1308+182	1.5, 2.0, 2.5, 3, 5 10, 15, 20, 30, 45, 60, 75, 90	44	0.40
1311−270	1.5, 2.0, 2.5, 5, 10, 15, 20, 30, 50, 70, 90	92	1.20
1318+113	0.5, 1.0, 1.5, 2.0, 2.5, 5, 10, 15, 20, 30, 50, 70, 90	180	0.40
1323+655	1.0, 1.5, 2.0, 2.5, 5, 10, 15, 20, 35, 50, 65, 80, 95	82	0.40
1334+119	1.5, 2.0, 2.5, 3, 5, 10, 15, 20, 35, 50, 65, 80, 95	39	0.50

TABLE II *(continued)*.

QUASAR	CONTOUR VALUES (percentage of peak brightness)	PEAK (mJy/beam)	BEAM (arcsec)
1345+584	1.0, 1.5, 2.0, 2.5, 5, 10, 15, 20, 30, 50, 70, 90	37	0.45
1354+258	1.0, 1.5, 2.0, 2.5, 5, 10, 15, 20, 30, 50, 70, 90	28	0.35
1456+092	0.5, 1.0, 1.5, 2, 5, 10, 15, 20, 35, 50, 65, 80, 95	170	0.40
1511+103	5, 10, 15, 20, 30, 50, 70, 90	17	1.20
1540+180	0.7, 1.2, 1.7, 2.2, 5, 10, 20, 35, 50, 65, 80, 95	157	0.40
1554−203	2.0, 2.5, 3.0, 3.5, 5, 10, 15, 20, 35, 50, 65, 80, 95	28	0.80
1557−199	4.0, 4.5, 5.0, 5.5, 6.0, 7.5, 10.0, 12.5, 15, 20, 25, 30, 45, 60, 75, 90	13	0.60
1559+173	1.5, 2.0, 2.5, 5, 10, 15, 20, 30, 50, 70, 90	238	0.38
1602−001	0.5, 1.0, 1.5, 2.0, 5, 10, 15, 20, 35, 50, 65, 80, 95	212	0.60
1629+120	1.0, 1.5, 2.0, 2.5, 5, 10, 15, 20, 35, 50, 65, 80, 95	251	0.40
1634+176	1.5, 2.0, 2.5, 3, 5, 10, 15, 20, 35, 50, 65, 80, 95	39	0.40
1658+575	2.0, 2.5, 3.0, 3.5, 5, 10, 15, 20, 35, 50, 65, 80, 95	35	0.40
1702+298	0.5, 1.0, 1.5, 2, 5, 10, 15, 20, 35, 50, 65, 80, 95	218	0.40
1732+160	2.0, 2.5, 3.0, 3.5, 5, 10, 15, 20, 35, 50, 65, 80, 95	47	0.50
1816+475	2.5, 5.0, 7.5, 10, 15, 20, 25, 35, 50, 65, 80, 95	22	0.40
1857+566	1.0, 1.5, 2.0, 2.5, 5, 10, 15, 20, 35, 50, 65, 80, 95	74	1.00
2025+117	6, 9, 12, 15, 20, 25, 30, 40, 50, 60, 70, 80, 90	18	2.00
2146−133	1.0, 1.5, 2.0, 2.5, 5, 10, 15, 20, 35, 50, 65, 80, 95	170	0.50
2149+212	0.5, 1.0, 1.5, 2, 5, 10, 15, 20, 30, 50, 70, 90	185	0.45
2150+053	0.5, 1.0, 1.5, 2.0, 2.5, 5, 10, 15, 20, 35, 50, 65, 80, 95	136	0.50
2156+297	0.5, 1.0, 1.5, 2, 5, 10, 15, 20, 30, 50, 70, 90	290	0.40
2158+101	0.7, 1.2, 1.7, 2.2, 2.7, 5, 10, 15, 20, 35, 50, 65, 80, 95	79	0.40
2209+152	2.0, 2.5, 3, 5, 10, 15, 20, 35, 50, 65, 80, 95	26	1.00
2222+051	1, 2, 3, 5, 10, 15, 20, 35, 50, 65, 80, 95	85	0.40
2223+210	1, 2, 3, 5, 10, 15, 20, 30, 50, 70, 90	899	0.40
2248+192	0.5, 1.0, 1.5, 2.0, 2.5, 5, 10, 15, 20, 30, 45, 60, 75, 90	110	0.40
2249+185	0.5, 1.0, 1.5, 2.0, 2.5, 5, 10, 15, 20, 25, 30, 45, 60, 75, 90	530	0.40
2332+489	2.0, 2.5, 3, 5, 10, 15, 20, 35, 50, 65, 80, 95	60	1.50
2338+042	0.8, 1.3, 1.8, 2.3, 2.8, 5, 10, 15, 20, 30, 45, 60, 75, 90	191	0.40
2345+061	0.7, 1.2, 1.7, 2.2, 2.7, 5, 10, 15, 20, 30, 45, 60, 75, 90	159	0.40
2354+144	0.5, 1.0, 1.5, 2, 5, 10, 15, 20, 35, 50, 65, 80, 95	246	1.00

TABLE III. — *Previously mapped steep spectrum high redshift quasars.*

QUASAR	RADIO SOURCE	z	REFERENCE
0017+154	3C 9	2.012	Swarup *et al.* 1982
1218+339	3C 270.1	1.519	Stocke *et al.* 1985
1258+404	3C 280.1	1.659	Swarup *et al.* 1982
1606+289	4C 28.40	1.989	Riley & Pooley 1975
2120+168	3C 432	1.805	Feigelson *et al.* 1984

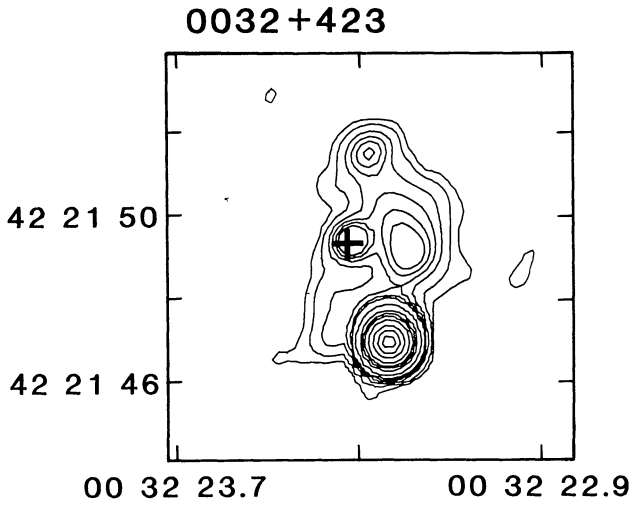

FIGURE 1.

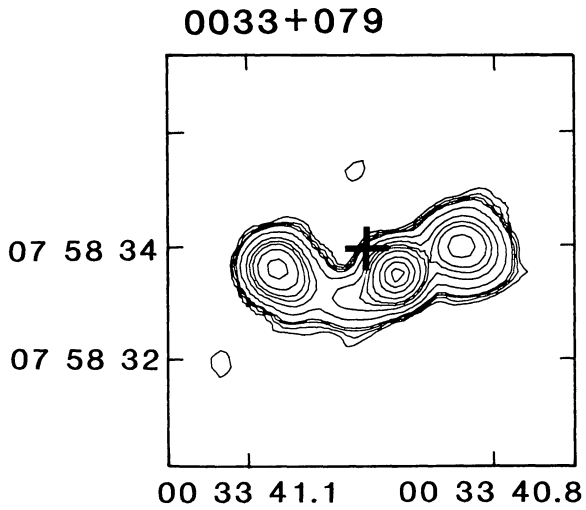

FIGURE 2.

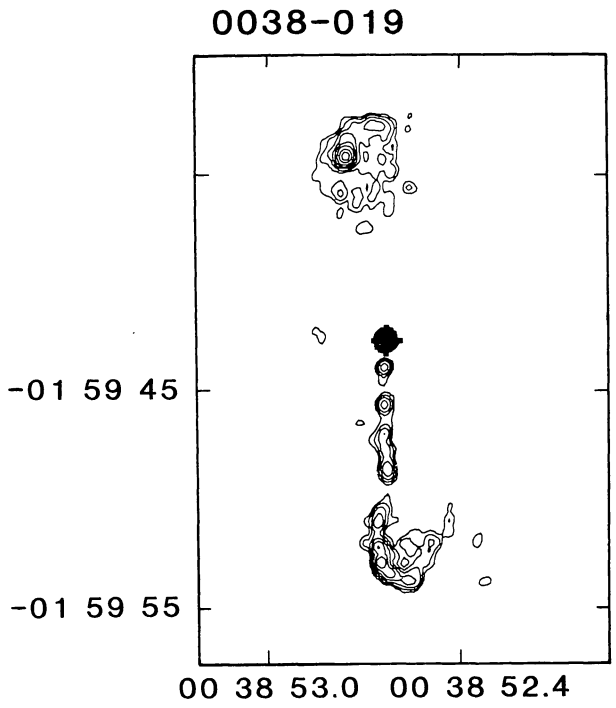

FIGURE 3.

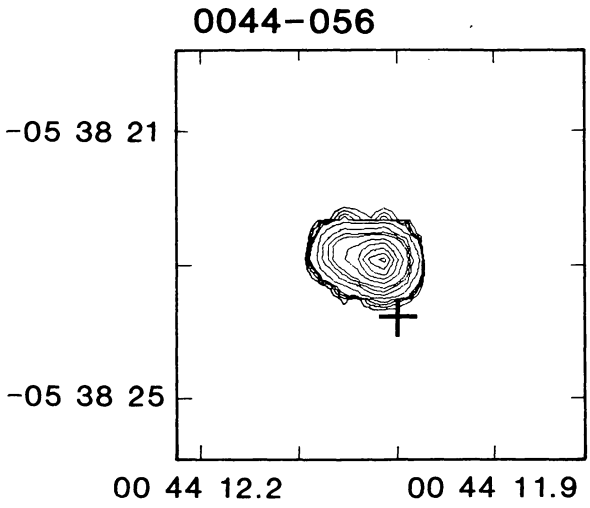

FIGURE 4.

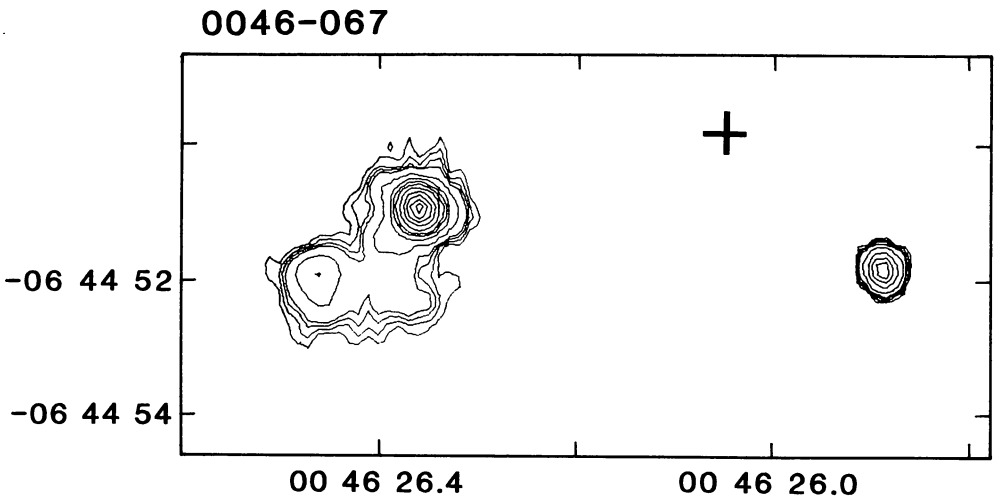

FIGURE 5.

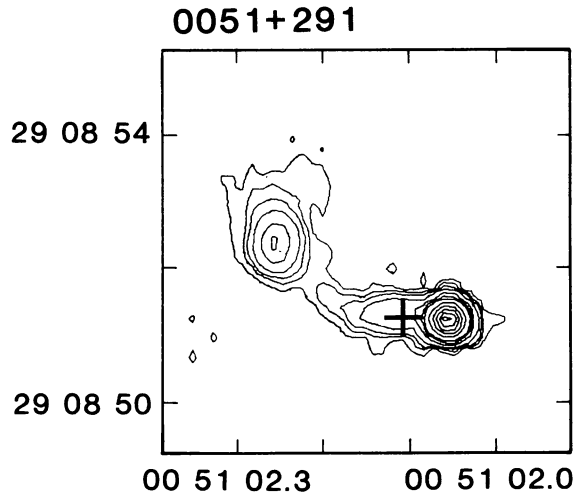

FIGURE 6.

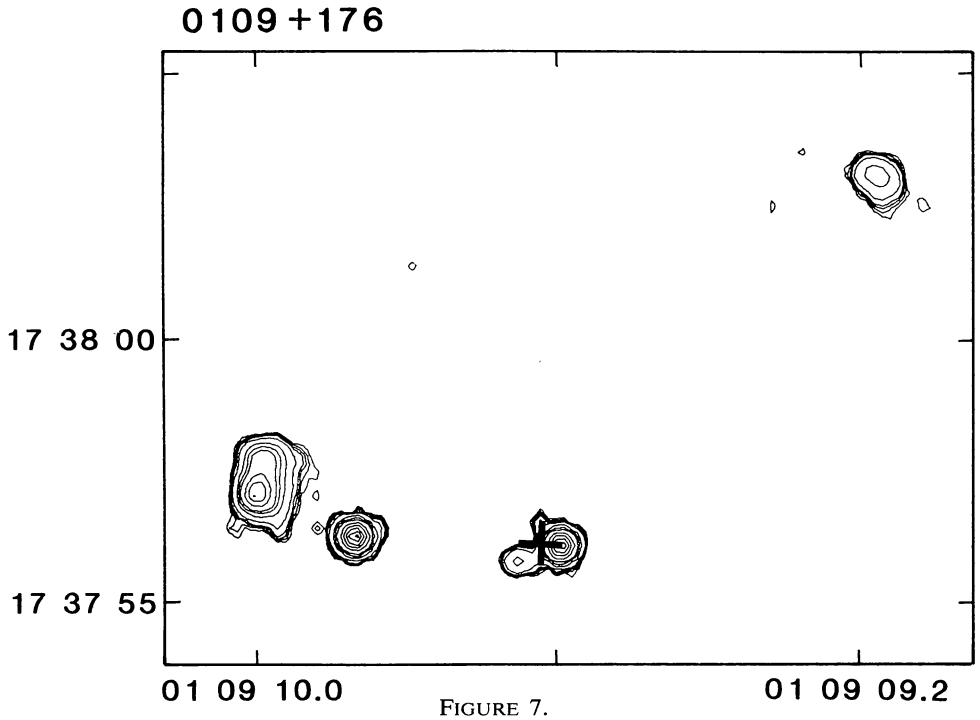

FIGURE 7.

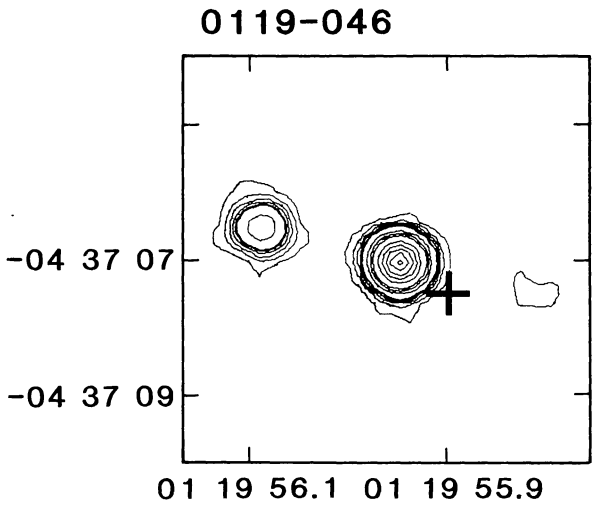

FIGURE 8.

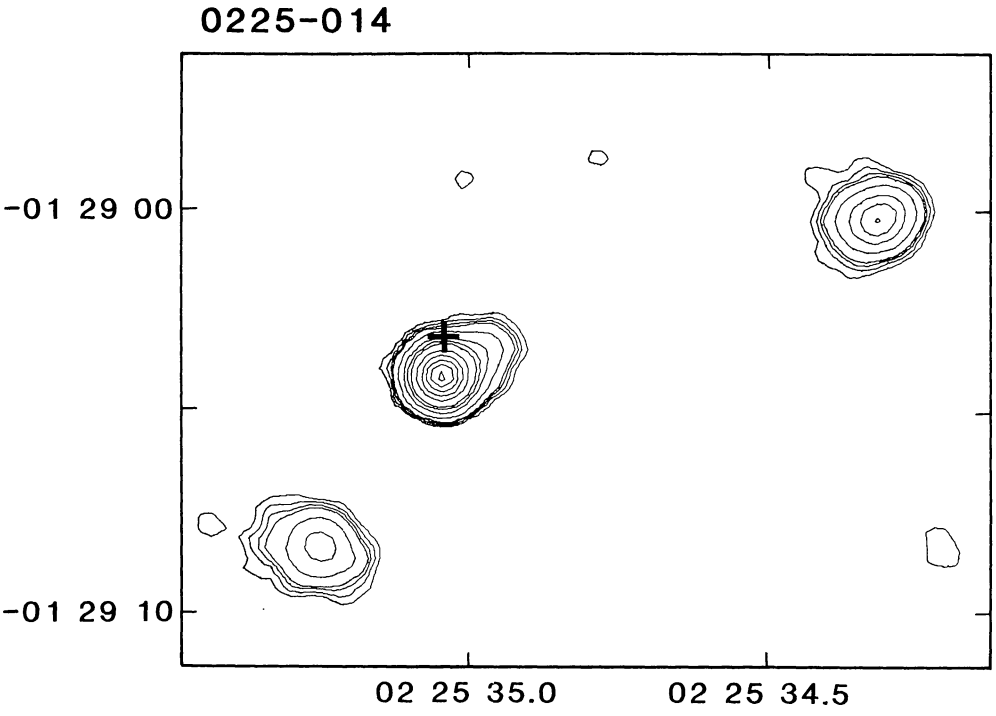

FIGURE 9.

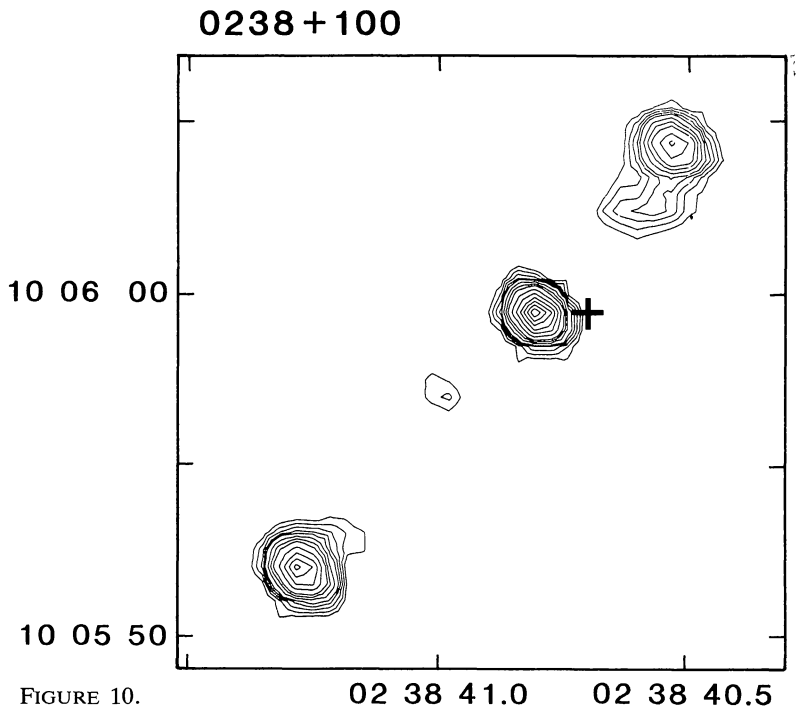

FIGURE 10.

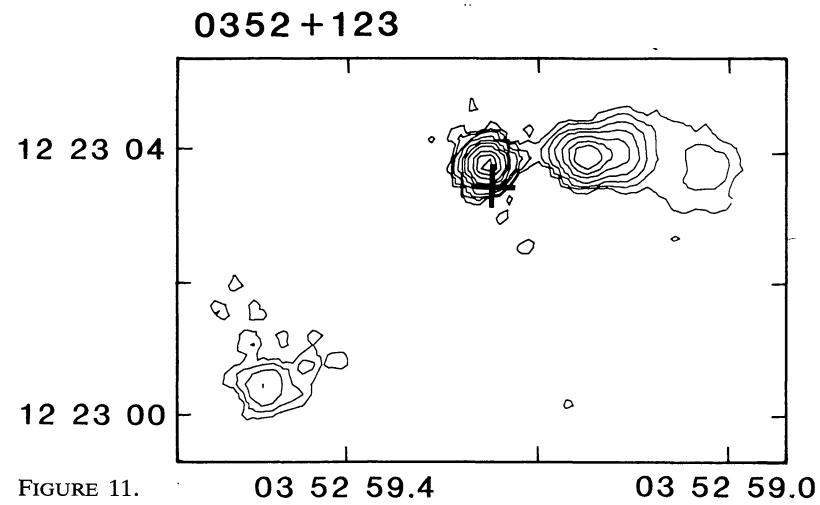

FIGURE 11.

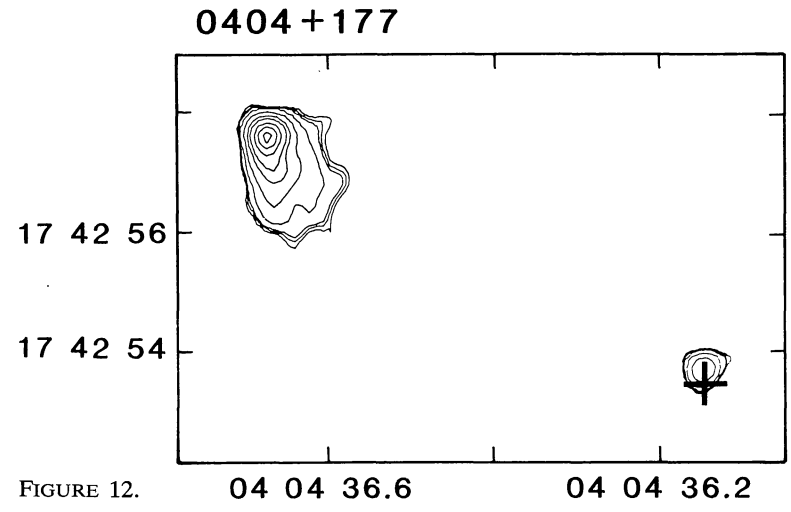

FIGURE 12.

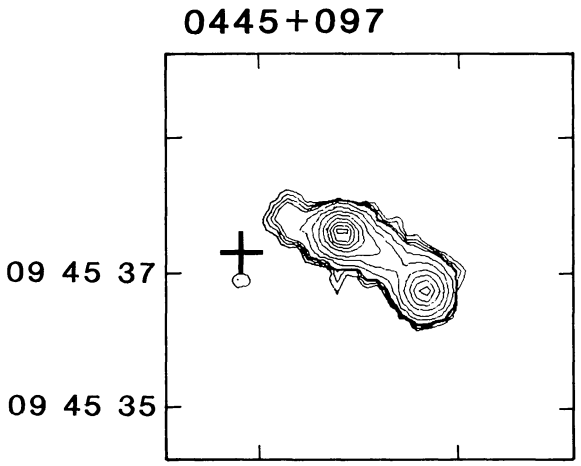

FIGURE 13.

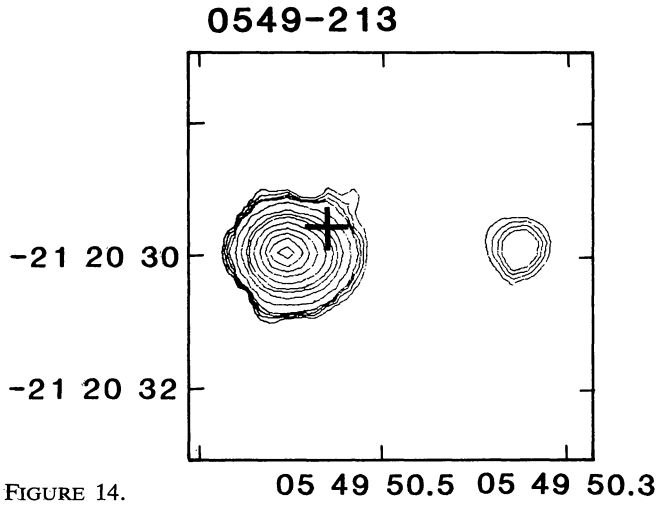

FIGURE 14.

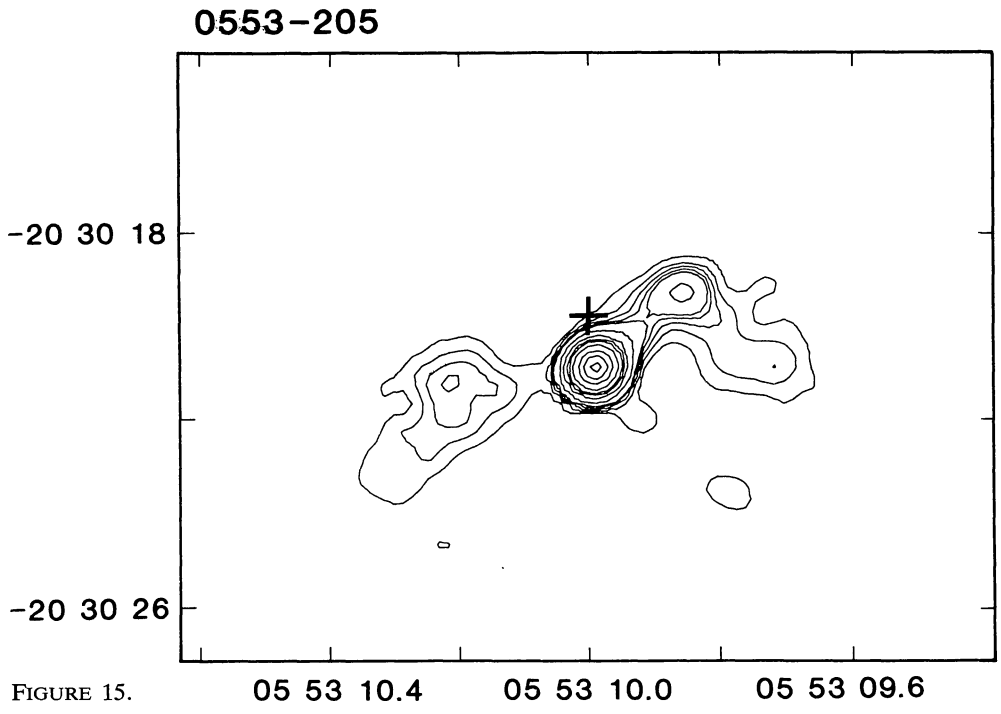

FIGURE 15.

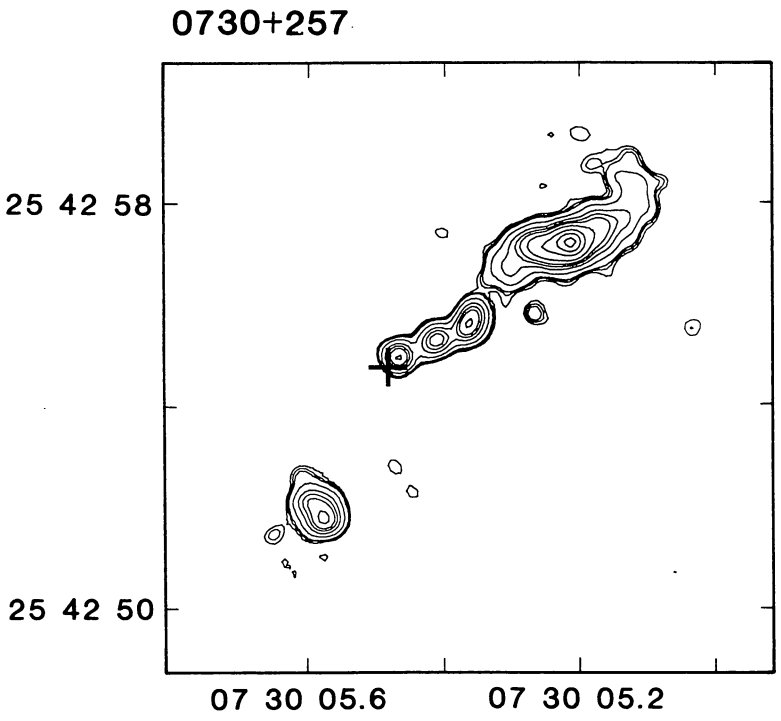

FIGURE 16.

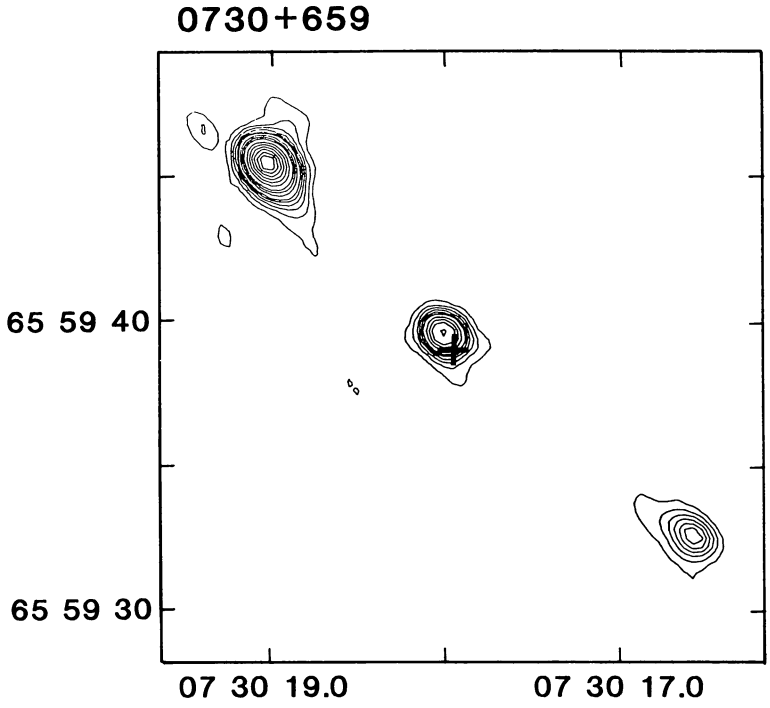

FIGURE 17.

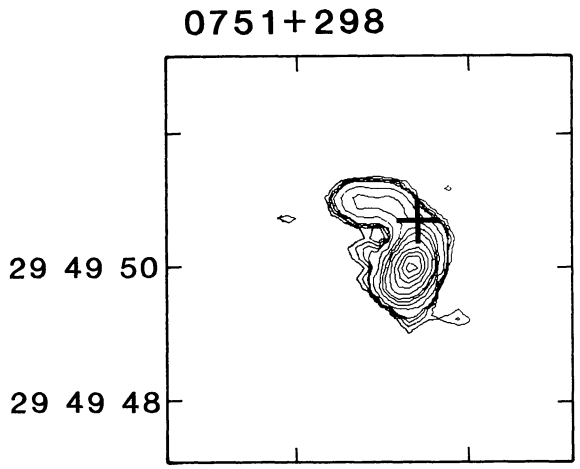

FIGURE 18.

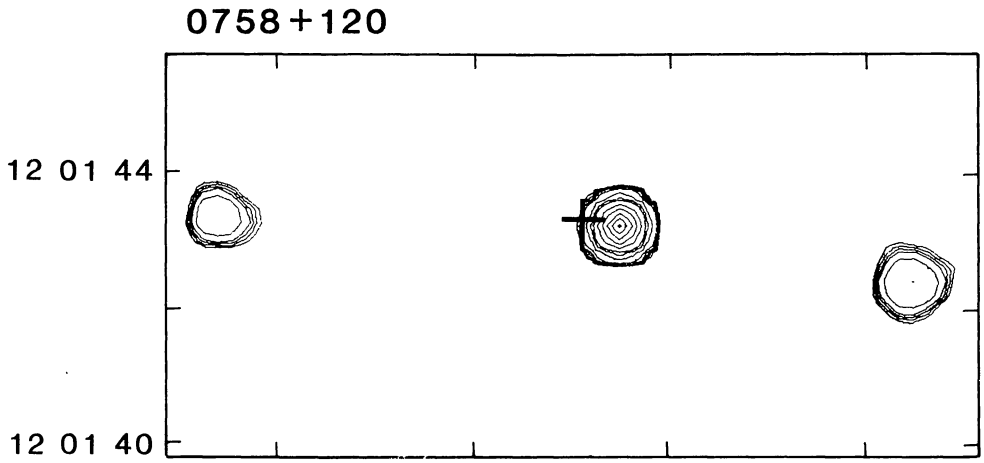

FIGURE 19.

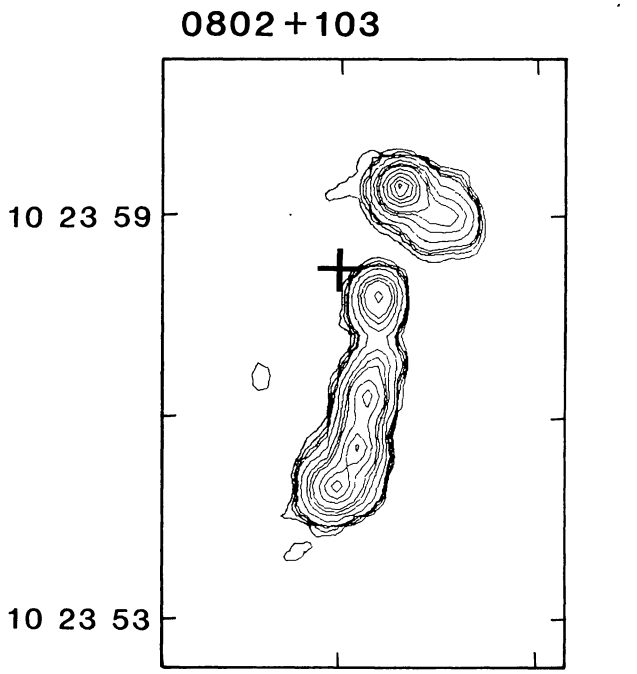

FIGURE 20.

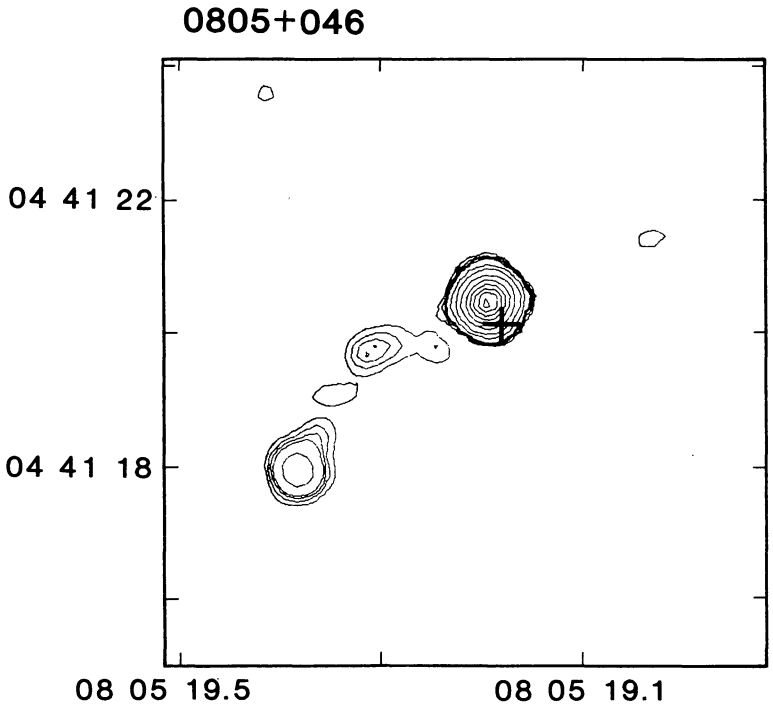

FIGURE 21.

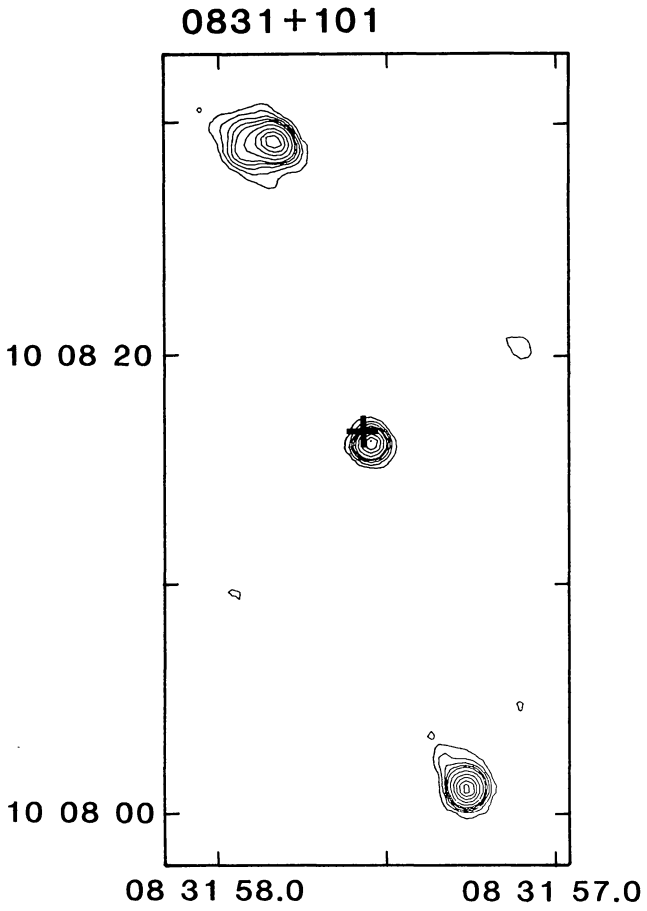

FIGURE 22.

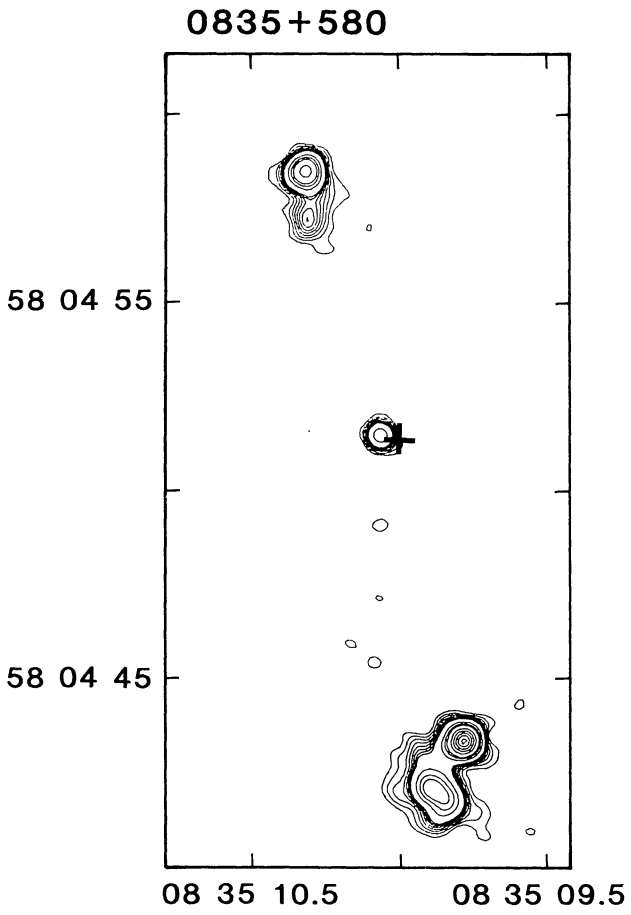

FIGURE 23.

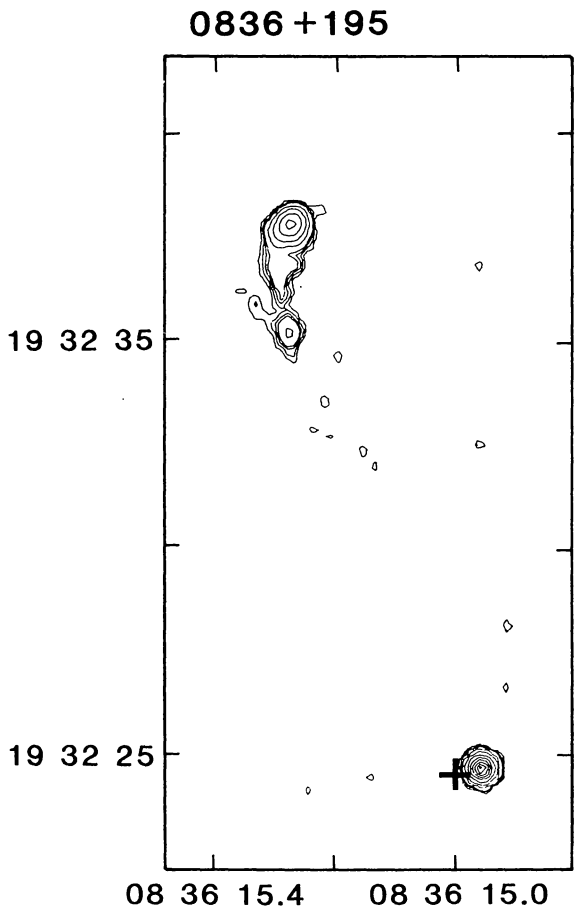

FIGURE 24.

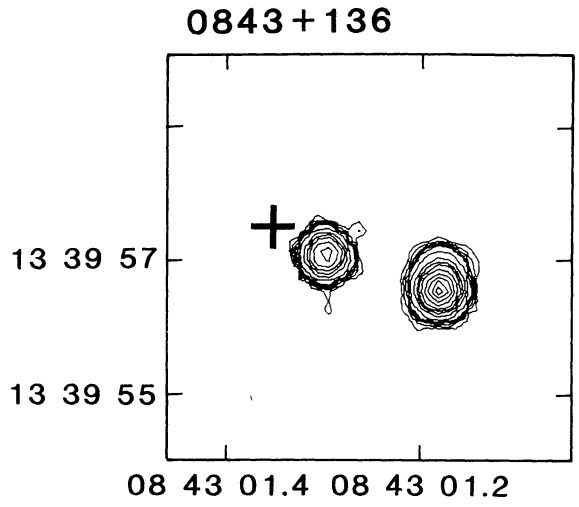

FIGURE 25.

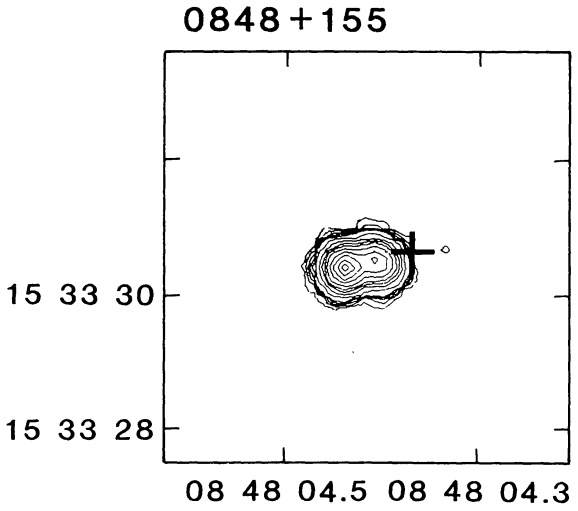

FIGURE 26.

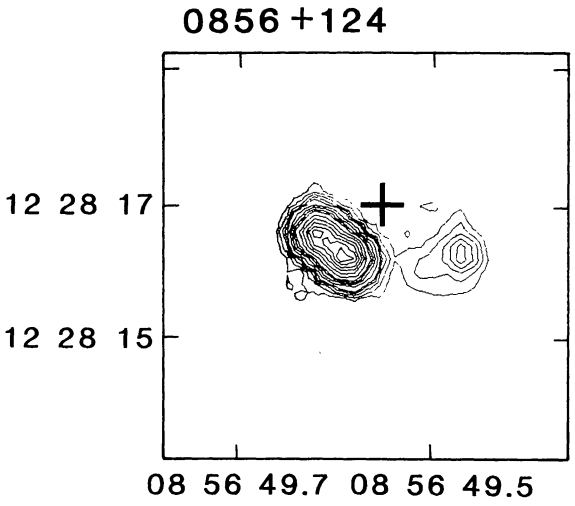

FIGURE 27.

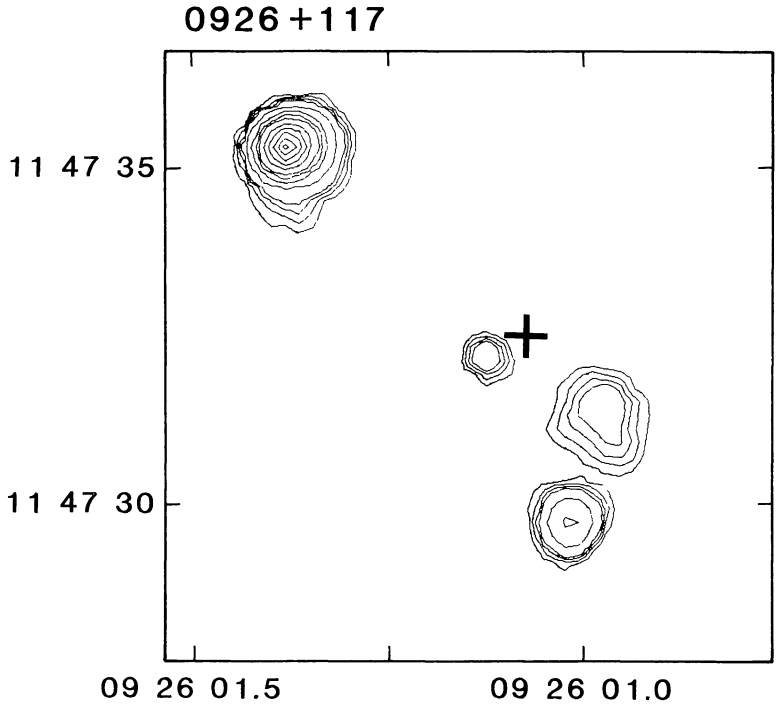

FIGURE 28.

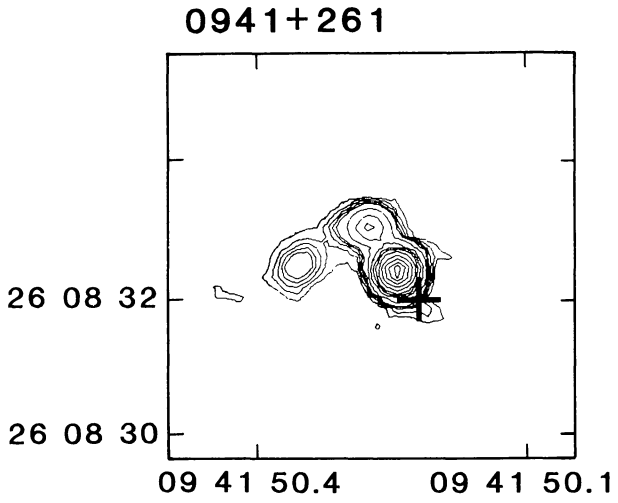

FIGURE 29.

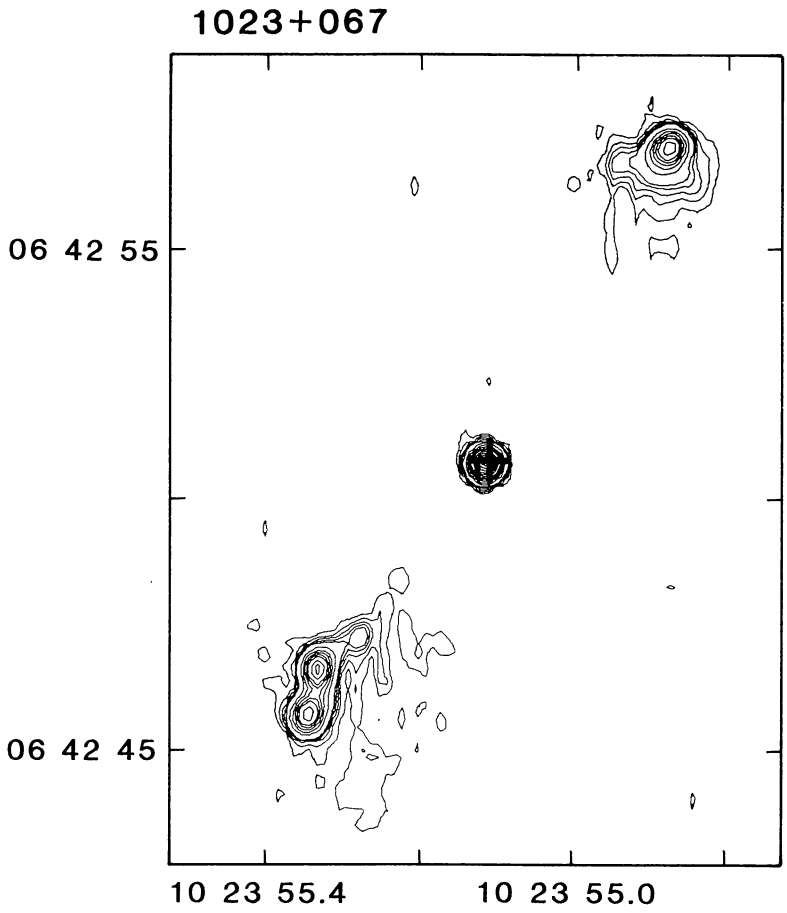

FIGURE 30.

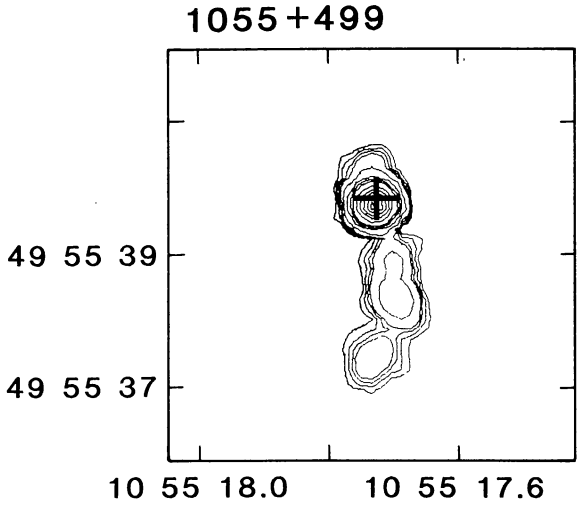

FIGURE 31.

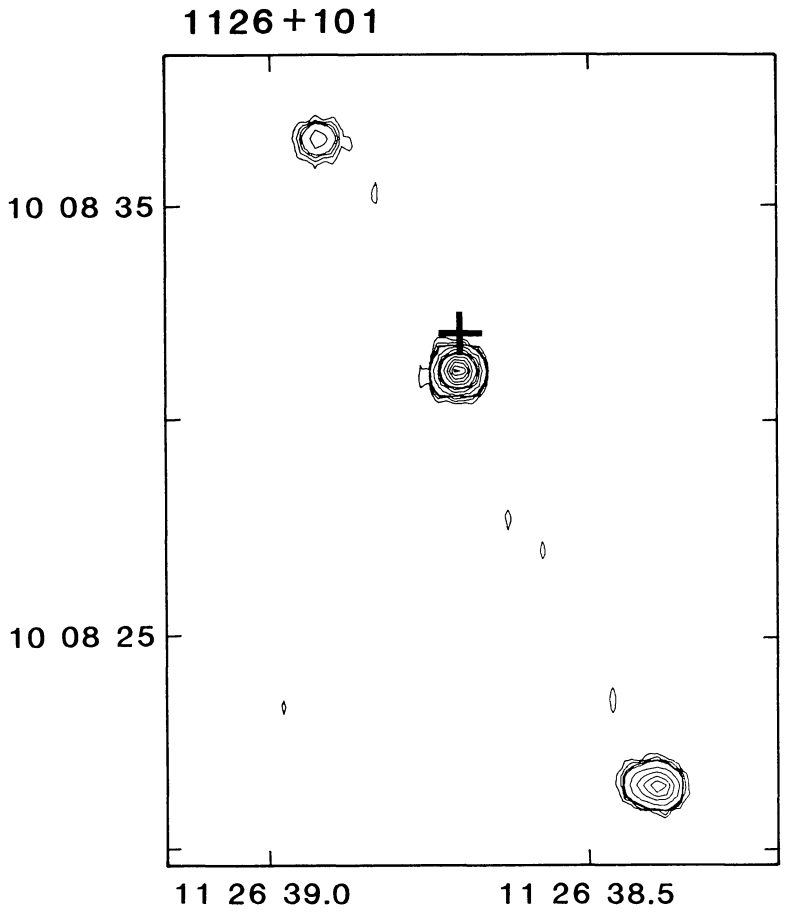

FIGURE 32.

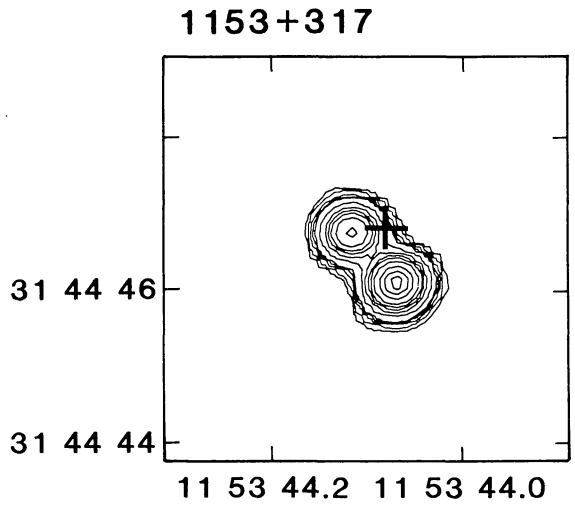

FIGURE 33.

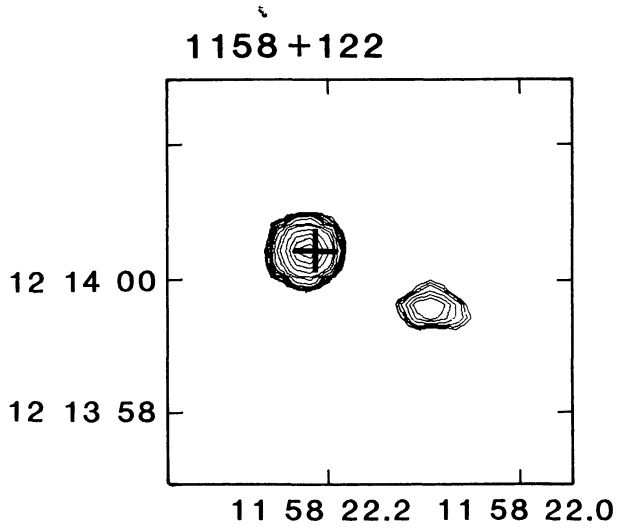

FIGURE 34.

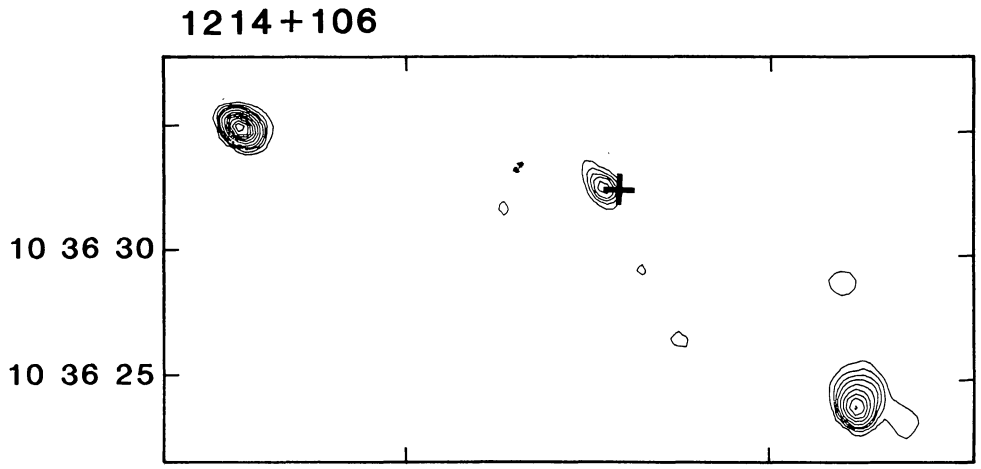

FIGURE 35.

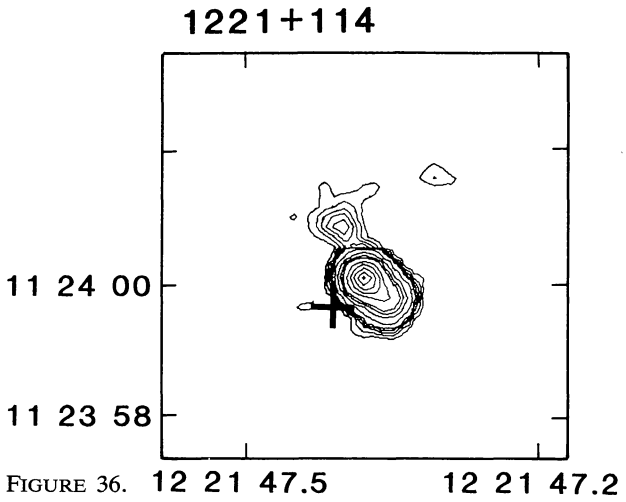

FIGURE 36.

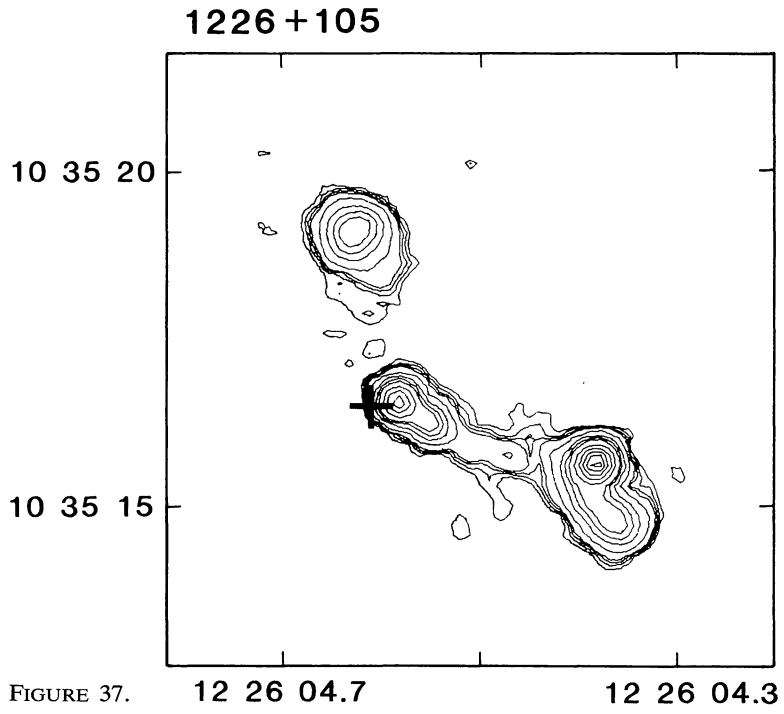

FIGURE 37.

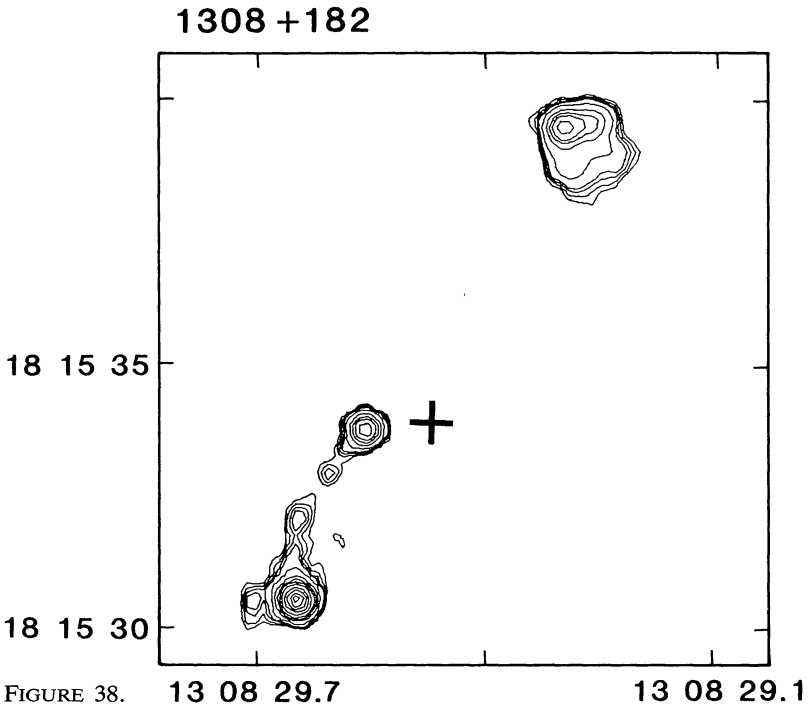

FIGURE 38.

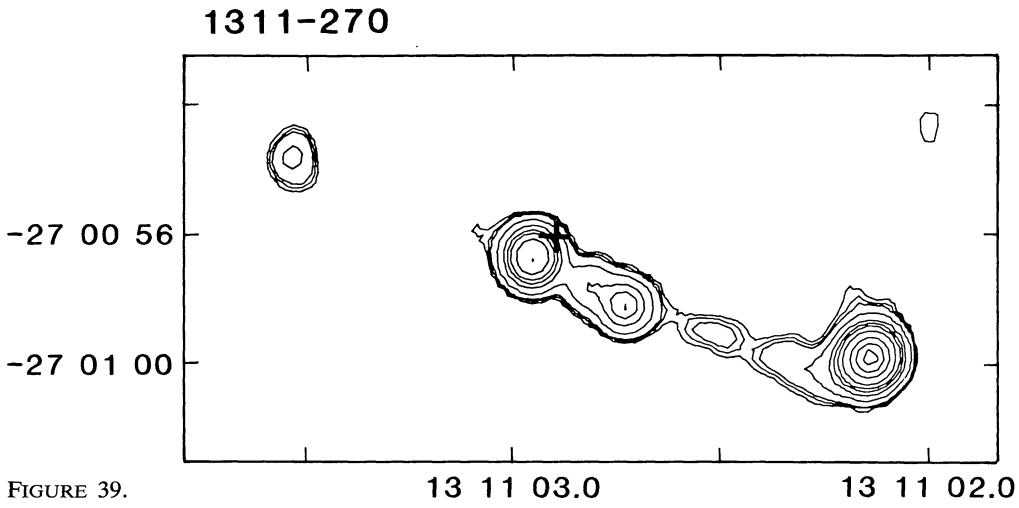

FIGURE 39.

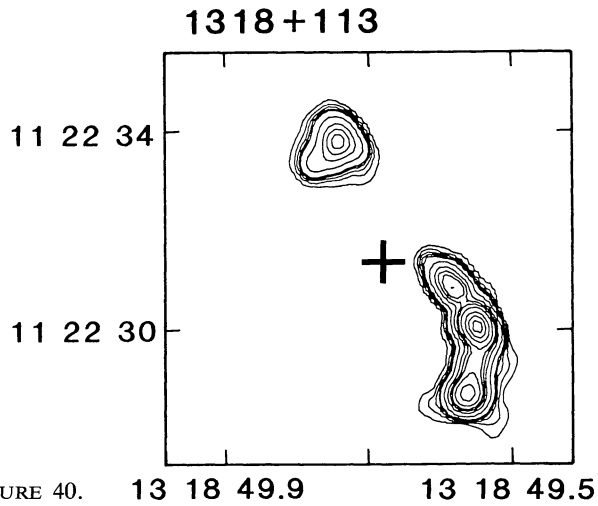

FIGURE 40.

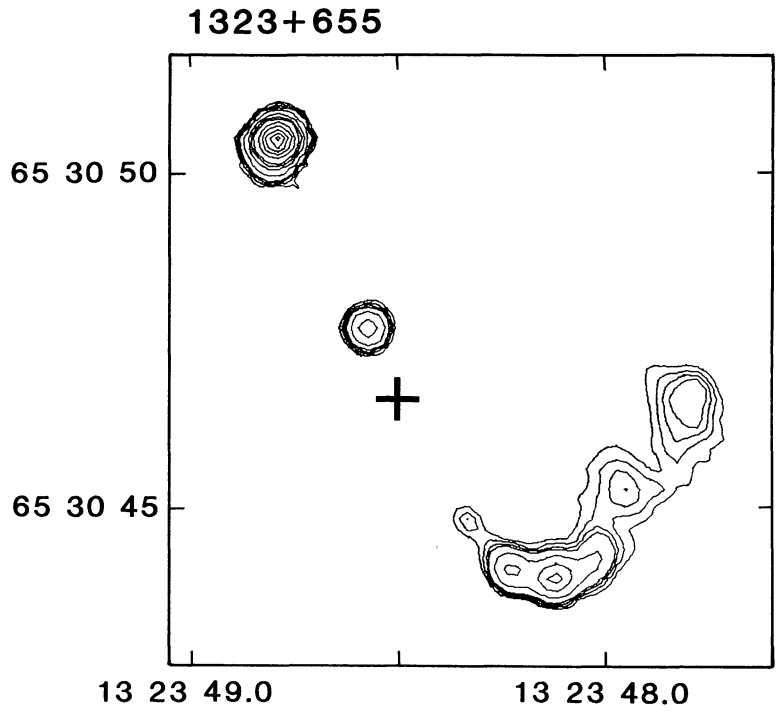

FIGURE 41.

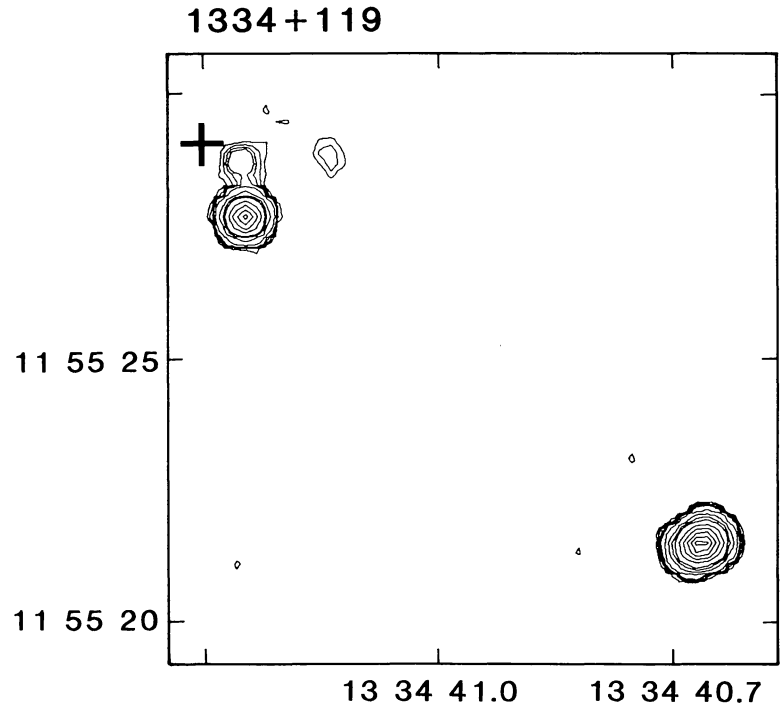

FIGURE 42.

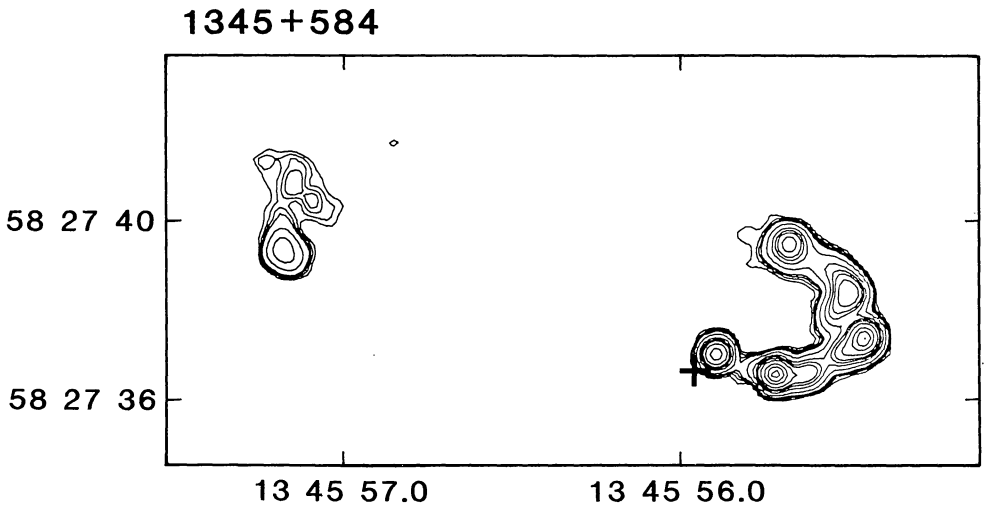

FIGURE 43.

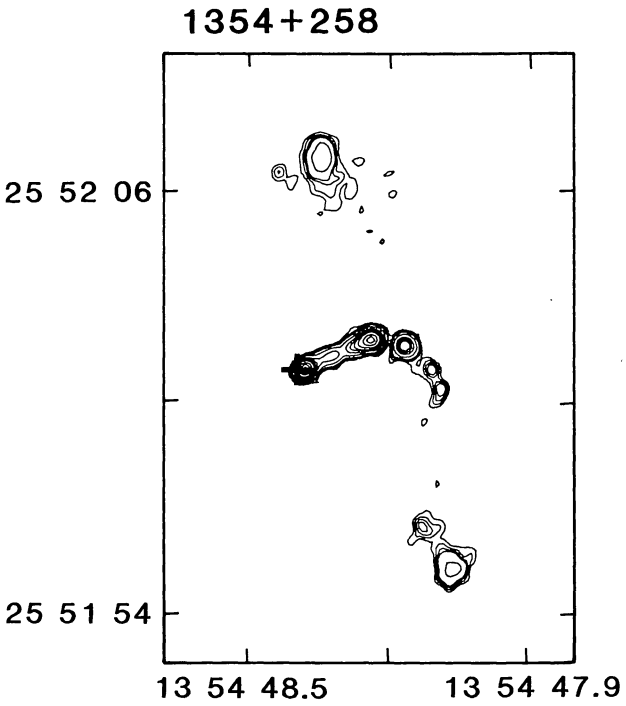

FIGURE 44.

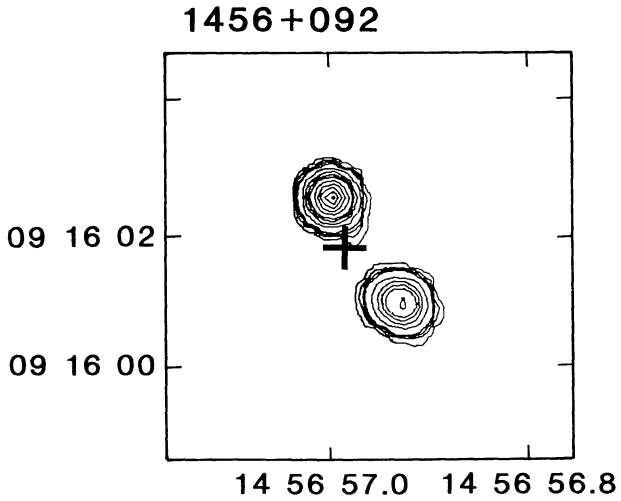

FIGURE 45.

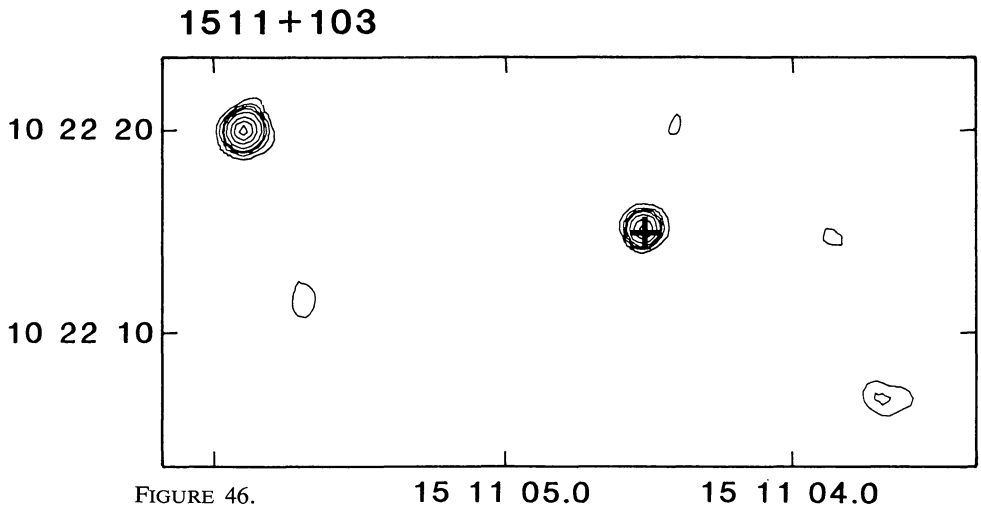

FIGURE 46.

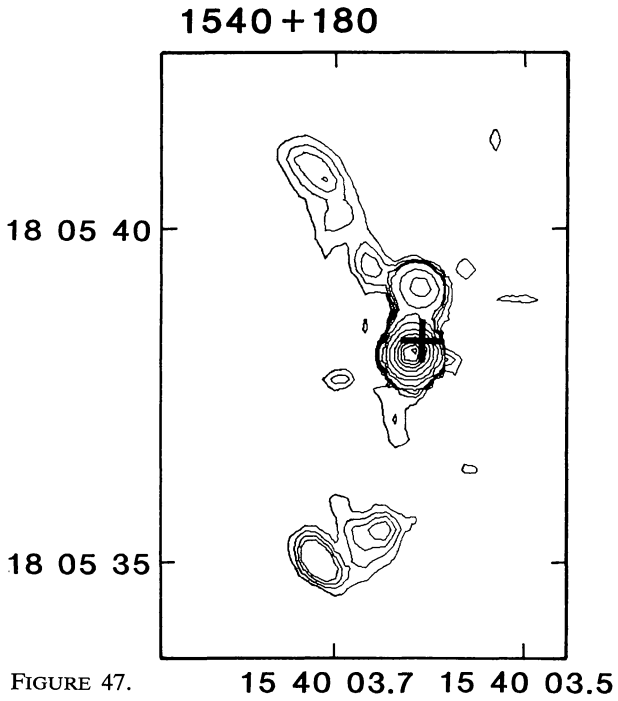

FIGURE 47.

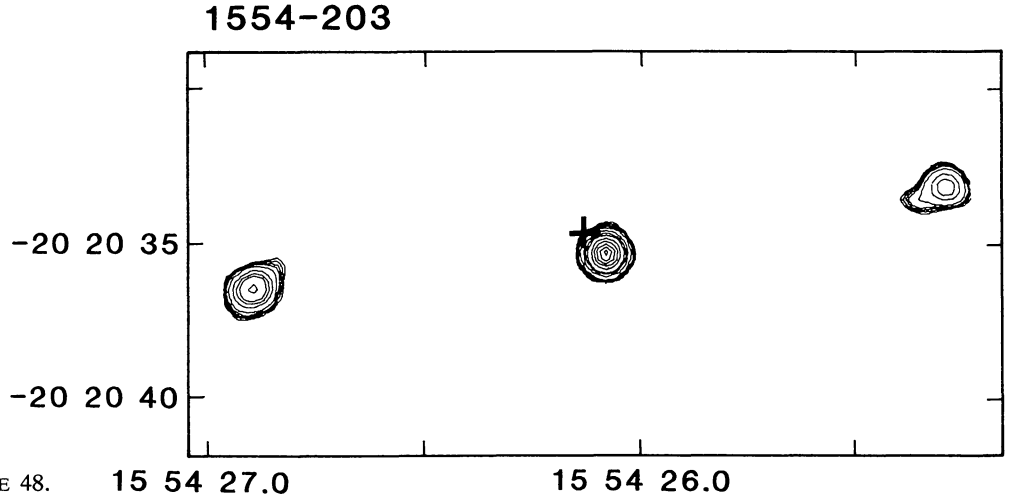

FIGURE 48.

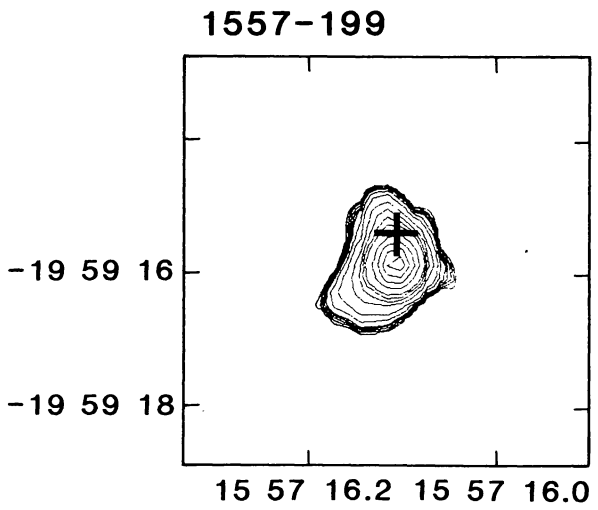

FIGURE 49.

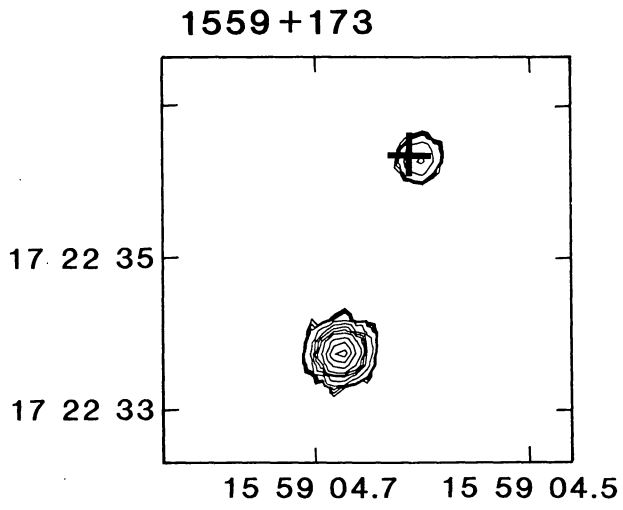

FIGURE 50.

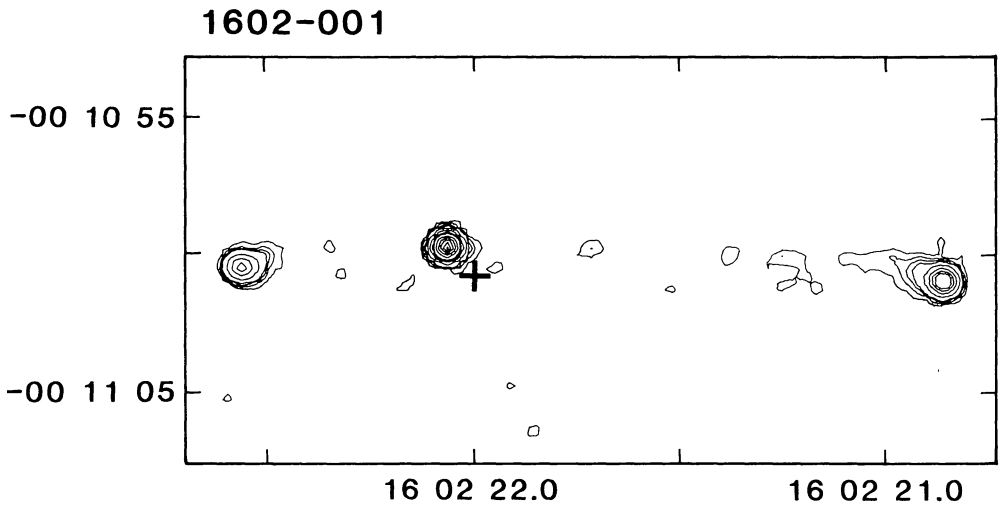

FIGURE 51.

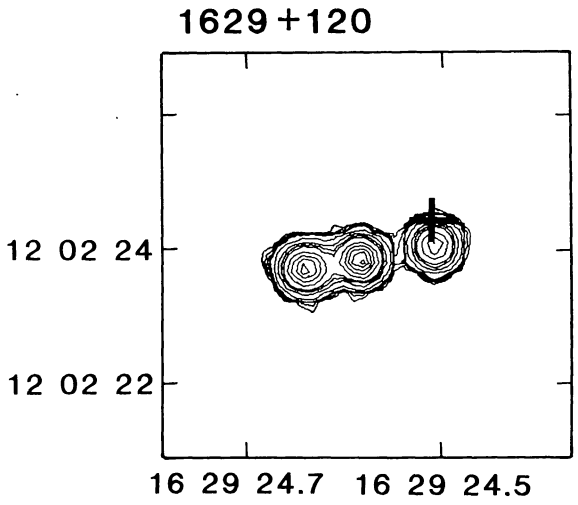

FIGURE 52.

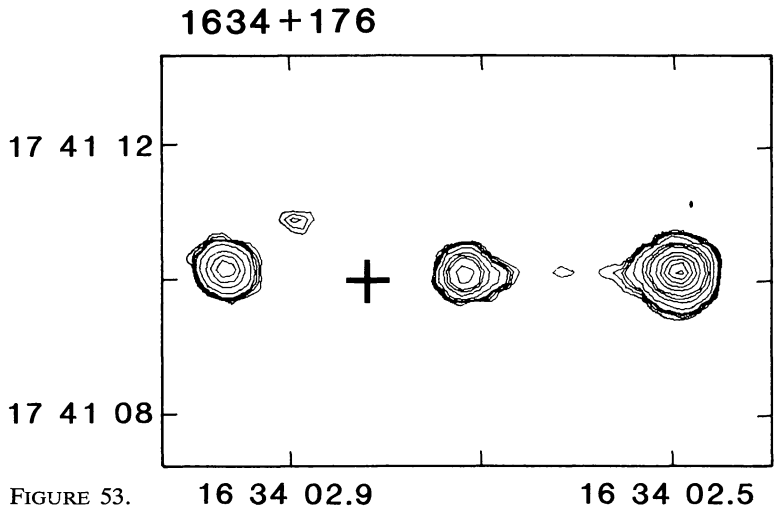

FIGURE 53.

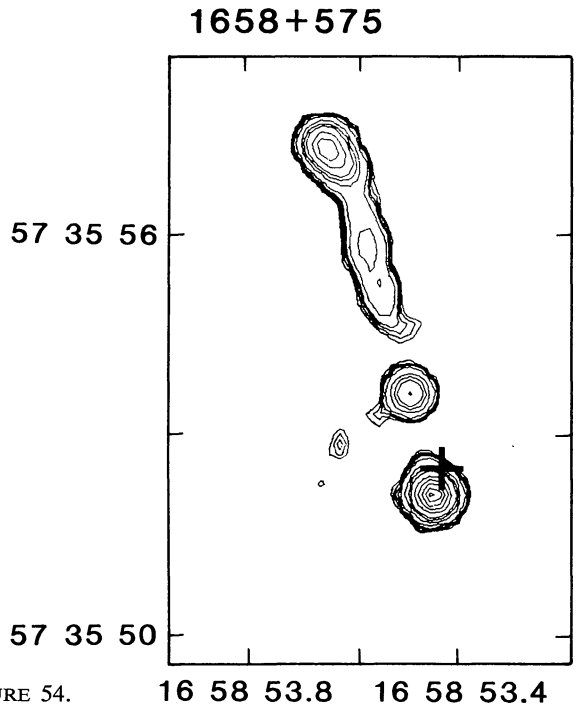

FIGURE 54.

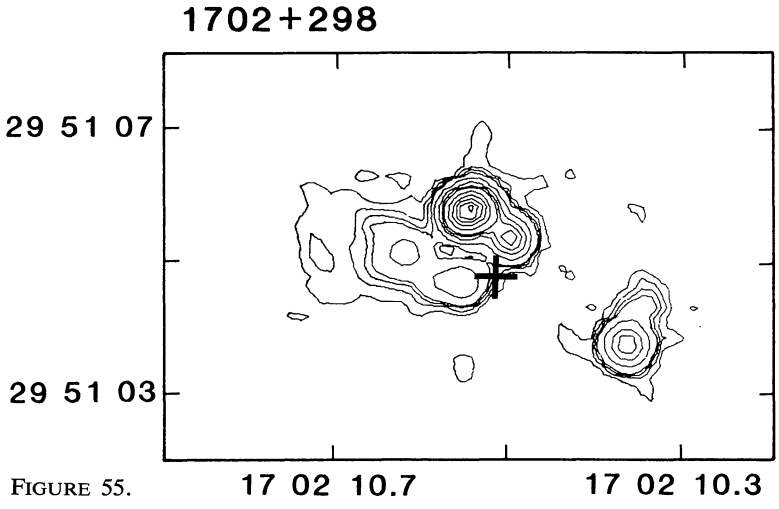

FIGURE 55.

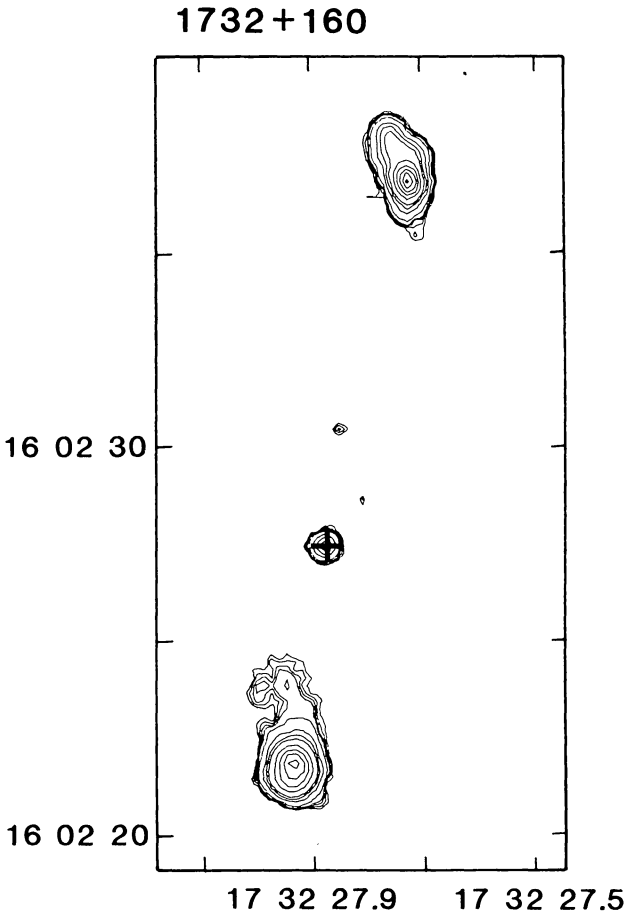

FIGURE 56.

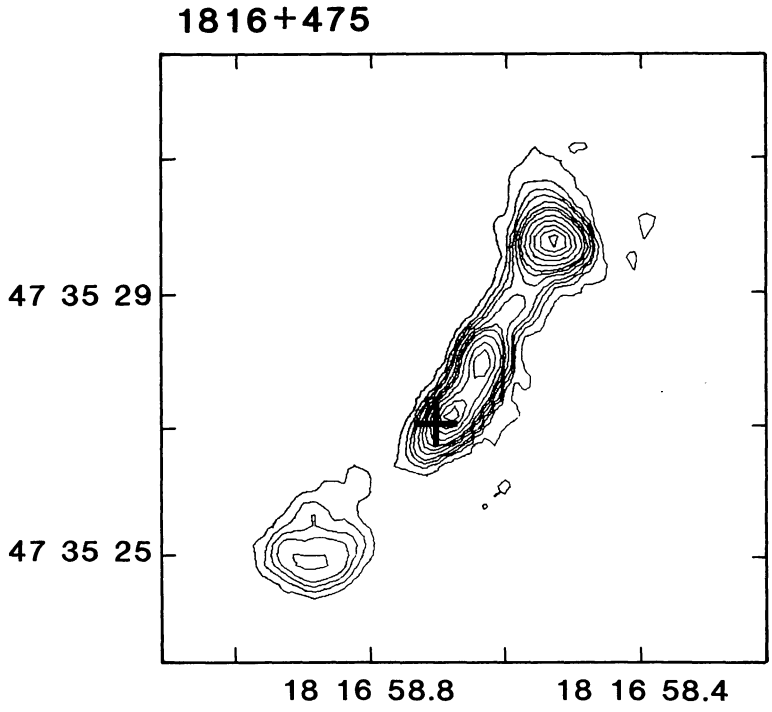

FIGURE 57.

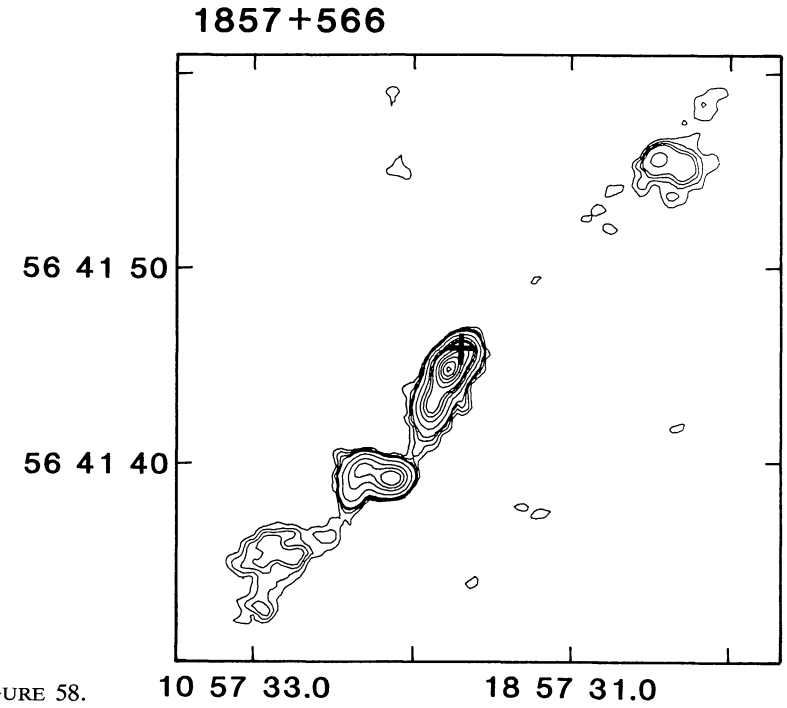

FIGURE 58.

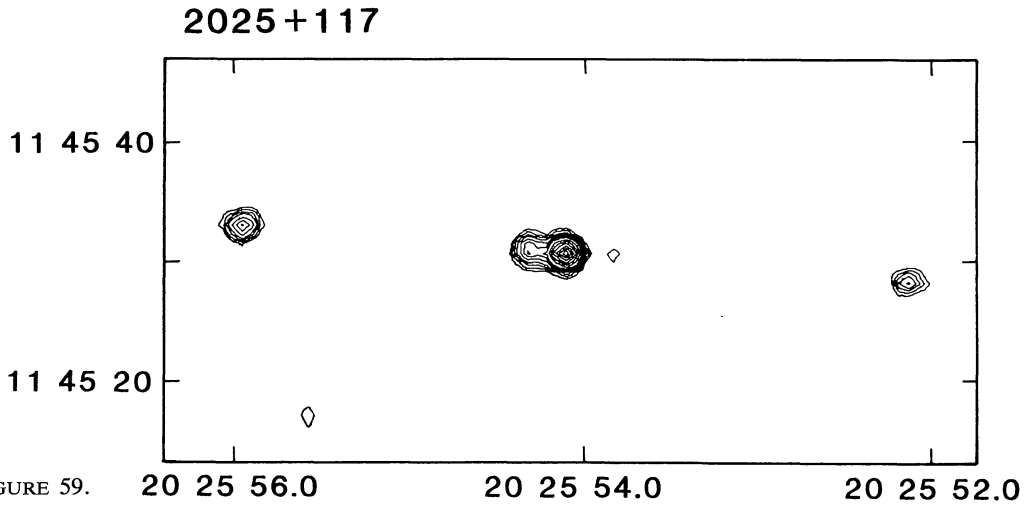

FIGURE 59.

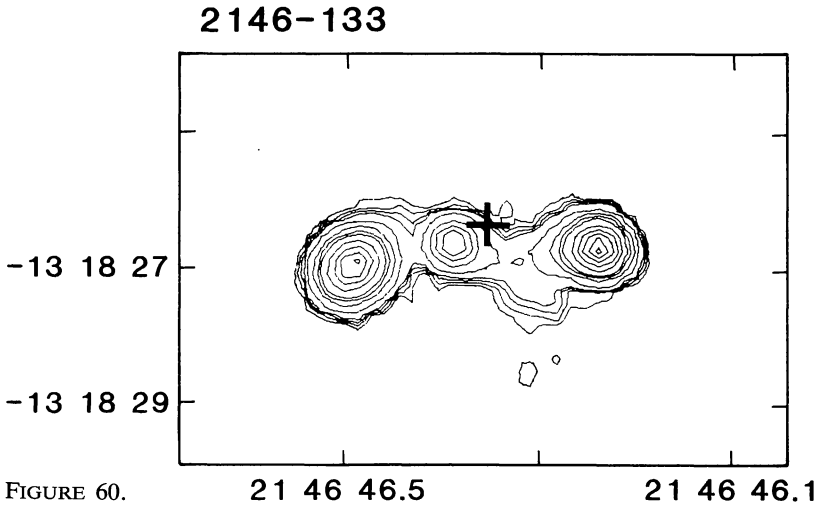

FIGURE 60.

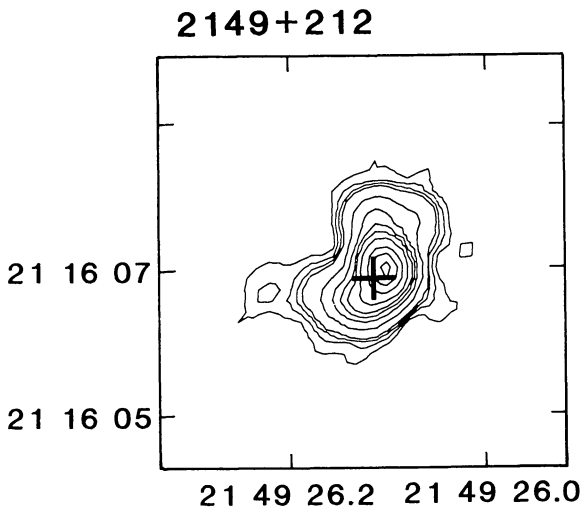

FIGURE 61.

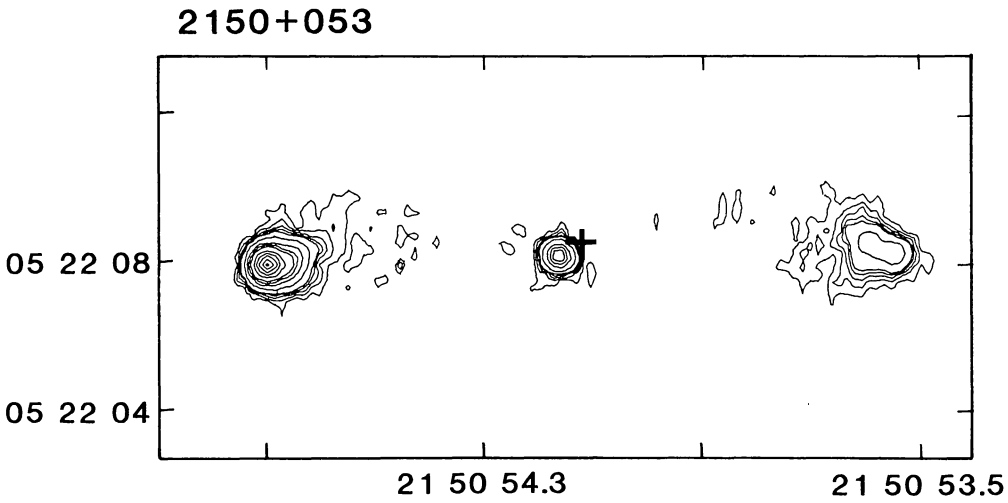

FIGURE 62.

FIGURE 63.

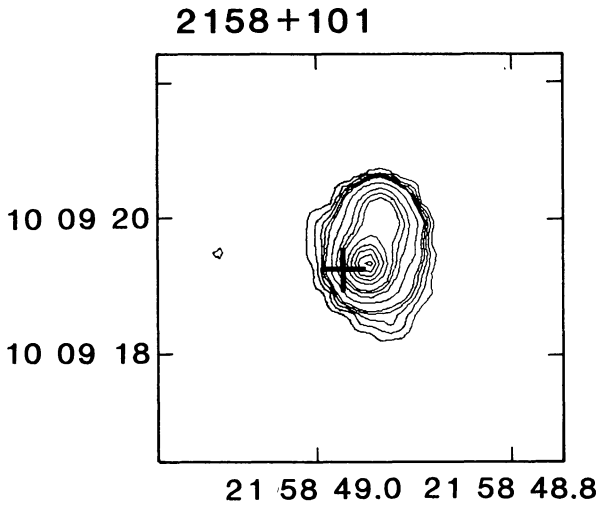

FIGURE 64.

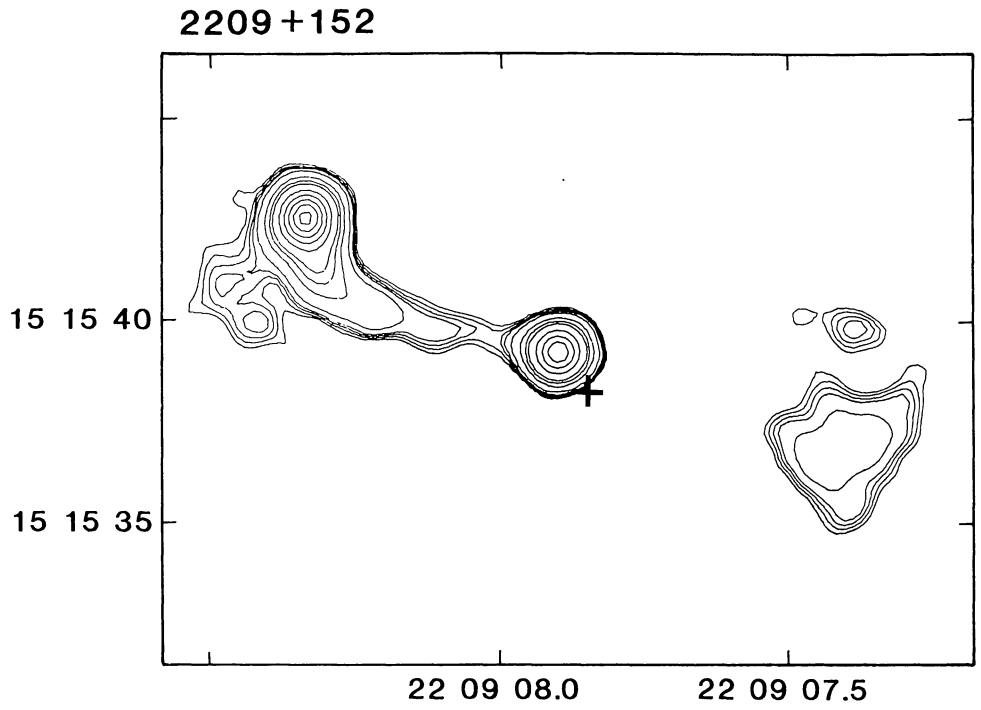

FIGURE 65.

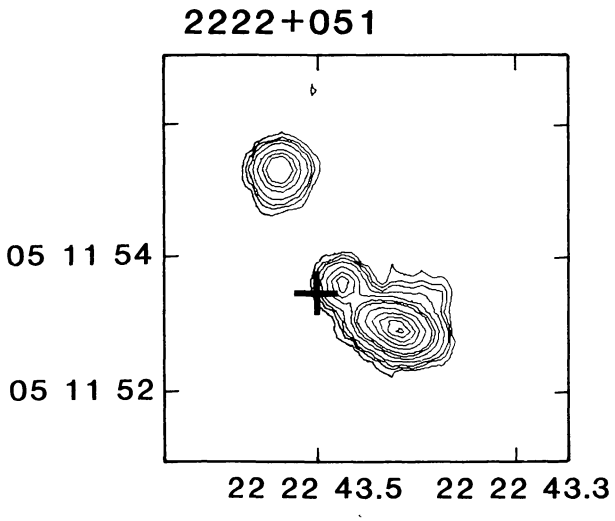

FIGURE 66.

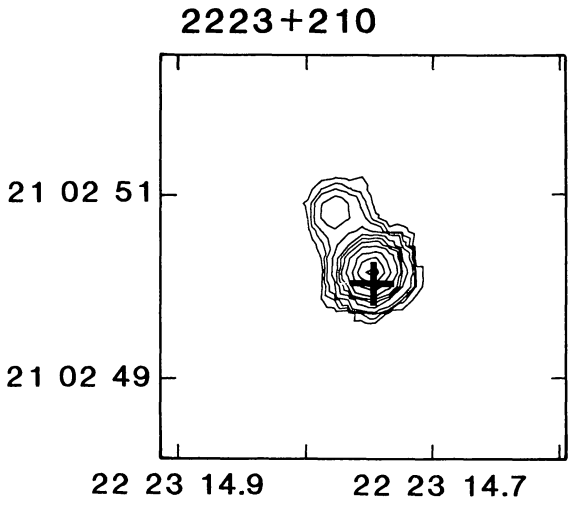

FIGURE 67.

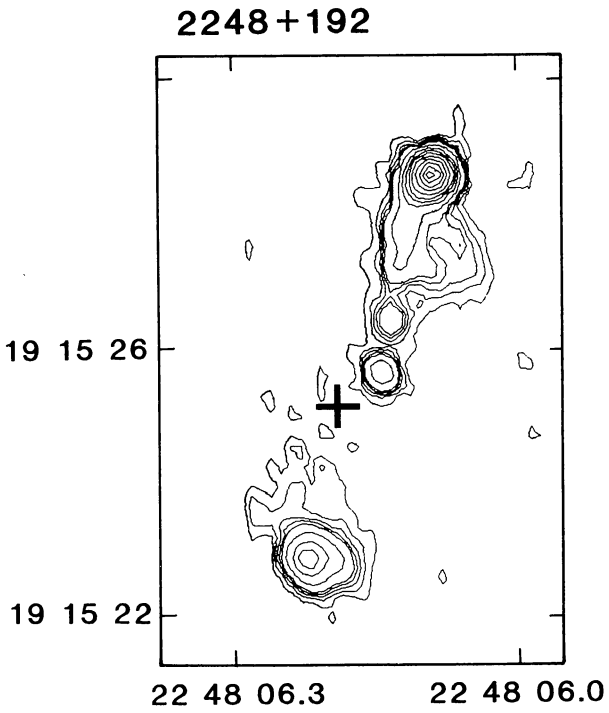

FIGURE 68.

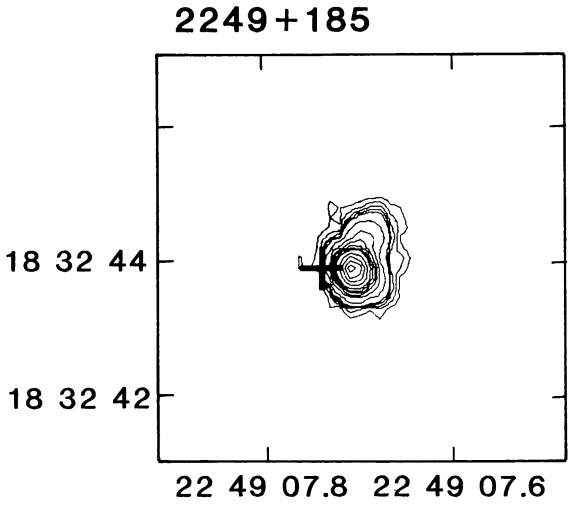

FIGURE 69.

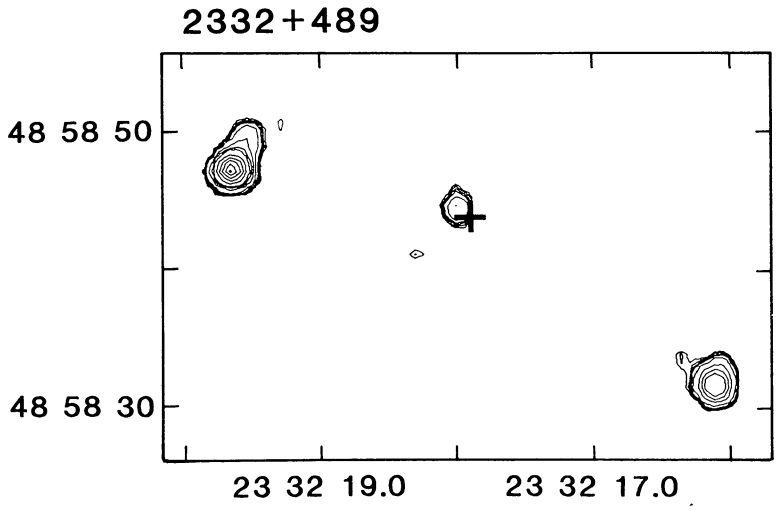

FIGURE 70.

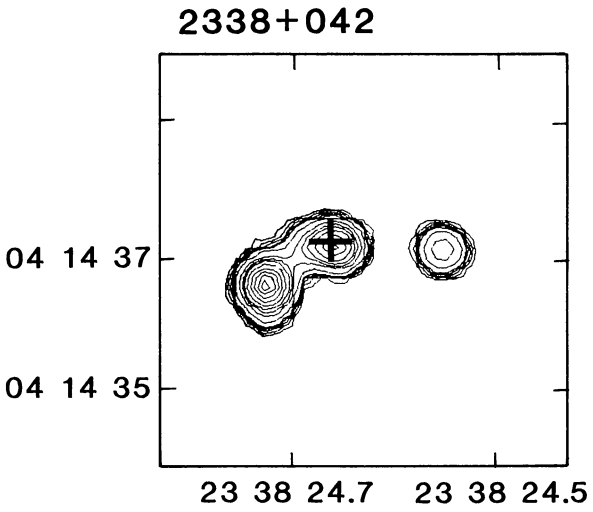

FIGURE 71.

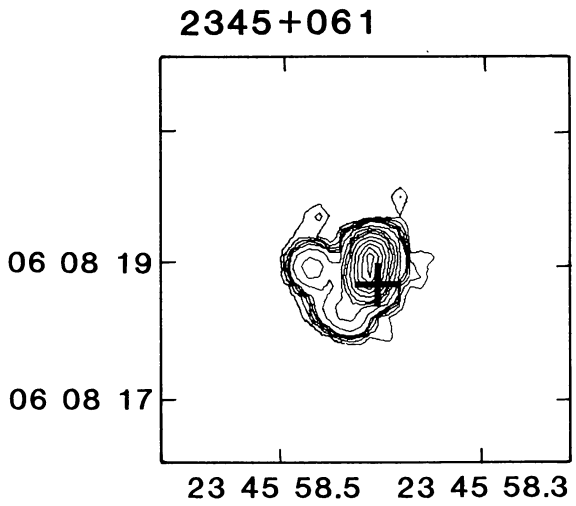

FIGURE 72.

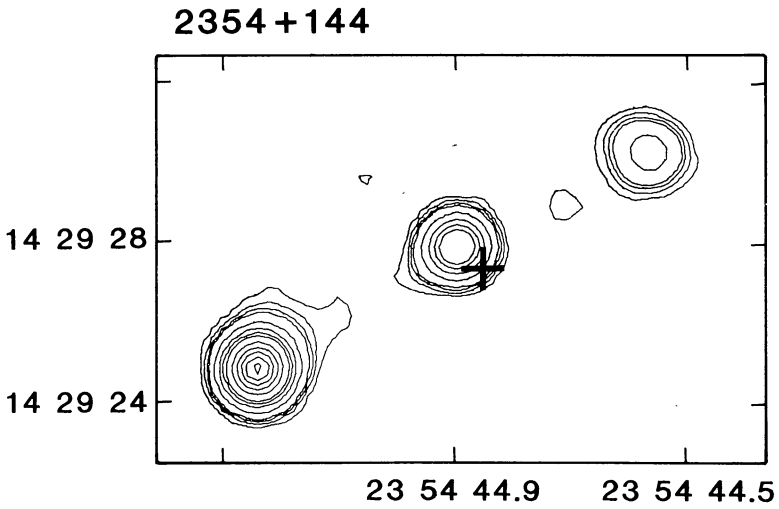

FIGURE 73.